AD-A154 829 NOTES ON UNSTEADY TRANSONIC CASCADE FLOWS(U) NIELSEN ENGINEERING AND RESEARCH INC MOUNTAIN VIEW CA D NIXON ET AL. 08 MAY 85 NEAR-TR-343 N00014-83-C-0435 1/1

UNCLASSIFIED F/G 20/4 NL

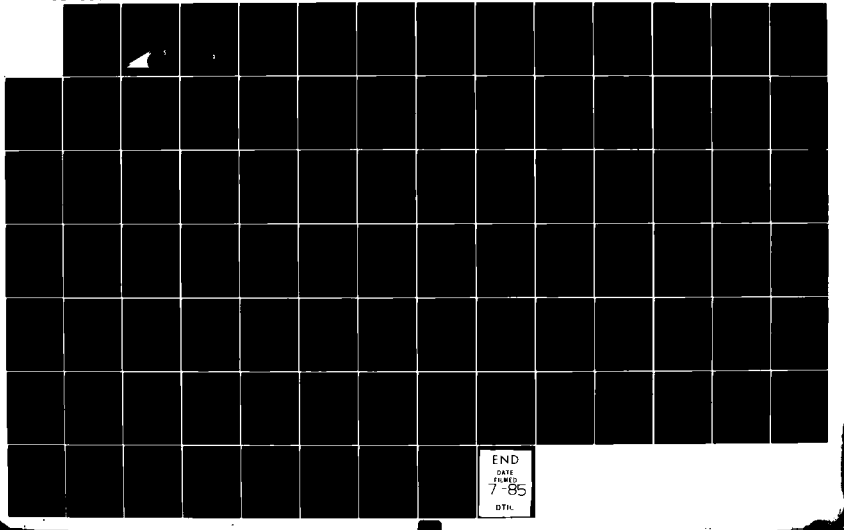

END
DATE FILMED
7-85
DTIC

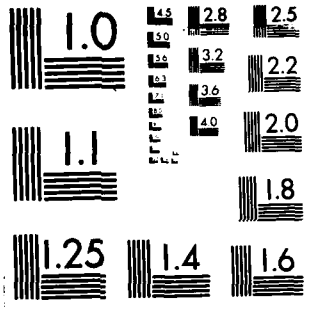

(7)

NOTES ON UNSTEADY TRANSONIC CASCADE FLOWS

by

David Nixon and Keh-Lih Tzuoo

for

OFFICE OF NAVAL RESEARCH
Arlington, VA 22217

NIELSEN ENGINEERING
AND RESEARCH, INC.

OFFICES: 510 CLYDE AVENUE / MOUNTAIN VIEW, CALIFORNIA 94043 / TELEPHONE (415) 968-9457

COPY NO. 13

NOTES ON UNSTEADY TRANSONIC CASCADE FLOWS

by

David Nixon and Keh-Lih Tzuoo

for

OFFICE OF NAVAL RESEARCH
Arlington, VA 22217

NEAR TR 343
April 1985

Prepared Under Contract No.

N00014-83-C-0435*

*The technical effort under the Office of Naval Research Contract No. N00014-83-C-0435 was funded by the Naval Air Systems Command.

NIELSEN ENGINEERING & RESEARCH, INC.
510 Clyde Avenue, Mountain View, CA 94043
Telephone (415) 968-9457

CURITY CLASSIFICATION OF THIS PAGE

REPORT DOCUMENTATION PAGE

REPORT SECURITY CLASSIFICATION: Unclassified	1b. RESTRICTIVE MARKINGS
SECURITY CLASSIFICATION AUTHORITY	3. DISTRIBUTION/AVAILABILITY OF REPORT: Unlimited Distribution
DECLASSIFICATION/DOWNGRADING SCHEDULE	
PERFORMING ORGANIZATION REPORT NUMBER(S): NEAR TR 343	5. MONITORING ORGANIZATION REPORT NUMBER(S)
6a. NAME OF PERFORMING ORGANIZATION: Nielsen Engineering & Research, Inc. / 6b. OFFICE SYMBOL (If applicable)	7a. NAME OF MONITORING ORGANIZATION: Office of Naval Research
6c. ADDRESS (City, State and ZIP Code): 510 Clyde Avenue, Mountain View, CA 94043	7b. ADDRESS (City, State and ZIP Code): 800 N. Quincy Street, Arlington, VA 22217
8a. NAME OF FUNDING/SPONSORING ORGANIZATION / 8b. OFFICE SYMBOL (If applicable)	9. PROCUREMENT INSTRUMENT IDENTIFICATION NUMBER: N00014-83-C-0435
8c. ADDRESS (City, State and ZIP Code)	10. SOURCE OF FUNDING NOS. — PROGRAM ELEMENT NO. / PROJECT NO. / TASK NO. / WORK UNIT NO.
11. TITLE (Include Security Classification): Notes on Unsteady Transonic Cascade Flows (U)	
12. PERSONAL AUTHOR(S): David Nixon, Keh-Lih Tzuoo	
13a. TYPE OF REPORT: Technical Report / 13b. TIME COVERED: FROM 9/12/83 TO 2/28/85	14. DATE OF REPORT (Yr., Mo., Day): May 8, 1985 / 15. PAGE COUNT: 76
16. SUPPLEMENTARY NOTATION	

COSATI CODES			18. SUBJECT TERMS (Continue on reverse if necessary and identify by block number)
FIELD	GROUP	SUB. GR.	Transonic Flow, Cascade Flow, Unsteady Flow
20	04		

19. ABSTRACT (Continue on reverse if necessary and identify by block number)

Several topics concerned with the unsteady transonic flow through cascades are considered. The indicial theory developed in previous work for cascade flows is examined and certain shortcomings eliminated. A consequence of this work is that some questions regarding the appropriate far field boundary conditions to use are raised. The "strong shock" potential theory previously developed for isolated airfoil flows has been incorporated into the cascade code.

A major topic in the present work is the examination of nonunique solutions for cascade flows. The variation of such solutions with cascade gap is studied with the conclusion that the nonunuique solutions are unlikely to occur for practical gap/chord ratios.

20. DISTRIBUTION/AVAILABILITY OF ABSTRACT: UNCLASSIFIED/UNLIMITED ☐ SAME AS RPT. ☒ DTIC USERS ☐	21. ABSTRACT SECURITY CLASSIFICATION
22a. NAME OF RESPONSIBLE INDIVIDUAL: George Derderian	22b. TELEPHONE NUMBER (Include Area Code): (202) 692-7444 / 22c. OFFICE SYMBOL

D FORM 1473, 83 APR EDITION OF 1 JAN 73 IS OBSOLETE.

SECURITY CLASSIFICATION OF THIS PAGE

TABLE OF CONTENTS

1. INTRODUCTION

An important problem in turbomachinery is the prediction of the flutter boundaries of the compressor. In order to compute these boundaries, the unsteady aerodynamic forces need to be understood. The aerodynamic causes of flutter in a compressor can be very complex, for example, the interaction between the flows induced by the rotor and stator. However, an important class of flutter is caused by a relatively simple aerodynamic flow due to the vibration of the blades on a given compressor row without the added complexity of exterior interactions. This latter problem is the simplest unsteady aerodynamic phenomenon of interest. In a compressor the oncoming velocity varies along the compressor blade, increasing from subsonic speeds at the hub to perhaps transonic speeds at the tip; it is the prediction of unsteady transonic flow in a compressor that is the most difficult. This report is concerned with the prediction of flutter in a vibrating compressor row when the flow is transonic.

The work reported here is concerned with solving the classic high frequency unsteady transonic small disturbance equation for cascade flows. A second topic is the validation of the cascade theory of Reference 1.

A major problem with potential theory is that it is not valid (Reference 2) when shock waves are present and, as a consequence, shock locations are not predicted adequately for medium to strong shock strengths, although the agreement for flows with weak shocks is acceptable. This disadvantage of the potential formulation can be overcome by modifying the theory to give the correct shock jump. This has been done by Nixon (Reference 3) for the steady transonic small disturbance (TSD) equation and by Kerlick, Nixon, and Ballhaus (Reference 4) for the unsteady low frequency equation. An extension of the

work in Reference 4 is reported in Reference 5 which is attached as Appendix 1.

Most of the numerical methods for predicting unsteady transonic flow stem from the work of Ballhaus and Goorjian (Reference 6), who developed an implicit algorithm to solve the low frequency TSD equation for isolated airfoils. An extension of this algorithm to high frequency motion was made by Rizzetta and Chin (Reference 7). For cascade flows a version of the Rizzetta-Chin algorithm was used by Kerlick and Nixon (Reference 8) to develop a method for cascade flows for unstaggered cascades. An alternative to the use of the unsteady TSD equation has been considered by Verdon and Caspar (Reference 9) who use a time linearized perturbation of the full potential equation for staggered and unstaggered cascades in a subsonic flow.

In a cascade flutter analysis the dominant parameter is the interblade phase angle which can determine the conditions at which the blade will flutter. In a numerical method, such as those discussed earlier, a flutter calculation can involve computing a test case for each value of the interblade phase angle. This is computationally expensive and, in order to reduce the cost, a technique developed by Nixon (Reference 1) may be used. This technique, which is based on indicial theory, decouples the cascade problem into a series of elementary problems, which are parametrically related, and only one solution need be computed. This elementary solution consists of a number of blades, all stationary with the exception of one blade which undergoes a step change. Once computed, the full unsteady solution for any frequency and interblade phase angle can be constructed by a judicious superposition.

In a previous report (Reference 10) the results obtained by the cascade code described in Reference 8 and the indicial method described in Reference 1 are examined. Several areas of concern arise in this examination. First, for a flat plate at subsonic conditions, the method of Kerlick and Nixon Reference 8 did not agree very well with the results of Verdon and Casper (Reference 9). Second, the indicial method did not give the super-resonance phenomena noted by Verdon and Casper. It is desirable that these points be clarified before further work is done. The question of super-resonance on the indicial method has been answered by including a (nominally) infinite number of blades in the cascade. This is done analytically rather than computationally.

In the above studies some questions regarding the far field boundary conditions used in cascade computations are raised. It is possible that the differences in the boundary conditions account for the difference in the flat plate results noted above. A discussion is given in the text.

In order to compute flows with strong shock waves the techniques of References 4 and 5 have been incorporated into the computer code. The details are given in Appendix 1.

The final issue to be addressed in the report is that of nonunique solutions. It has been known for some years that the potential equation gives nonunique solutions (References 11, 12) for isolated airfoils. It is established here that these solutions also occur for steady cascade flows. For unsteady flows the unsteady perturbation seems to be unique although the perturbation is around an artificial value of lift. These computations are for a reduced frequency of unity and is in

agreement with the results of Williams et al. (Reference 13) for isolated airfoils. However, for low frequencies an artificial behavior is evident for isolated airfoils (Reference 13) and may occur for cascade flows.

The analyses of Steinhoff and Jameson (Reference 11), Salas et al. (Reference 12), and Williams et al. (Reference 13) are essentially numerical experiments. Nixon (Reference 14) has attempted a more analytic study of the problem. Reference 14 is attached as Appendix 2. In Reference 14 Nixon has shown that for isolated airfoils there is the possibility of multiple solutions due to the presence of eigensolutions in the equations. There does not seem to be any way to avoid these solutions; in fact it is indicated that a stable algorithm helps the appearance of the eigensolutions. In the present work the analysis of Reference 14 is extended to include steady cascade effects. It is found that the effect of the eigensolutions varies as the inverse square of the gap. It is likely that for practical cascade flows the nonunique solutions do not arise.

2. COMMENTS ON THE ACCURACY OF THE NEAR CASCADE CODE

In the previous work on this contract, reported in Reference 10 a discrepancy between the results of the computer code CTRAN, developed under Contract N00018-81-C-0169, and the code of Verdon and Casper (Reference 9) for the subsonic flow through a cascade of flat plates was noted. Since the flat plate is a classical case this is a disturbing error. Hence some thought has been given as to the reasons for the disagreement.

For subsonic flows the Verdon and Caspar equation is equivalent to the small disturbance equation

$$(1-M_\infty^2\cos^2\theta)\ \phi_{xx} + (1-M_\infty^2\sin^2\theta)\phi_{yy} - \frac{2cM_\infty^2\cos\theta}{U_\infty}\ \phi_{xt} - 2\ M_\infty^2\sin\theta\cos\theta\phi_{xy}$$

$$- \frac{2cM_\infty^2\sin\theta}{U_\infty}\ \phi_{yt} - \frac{M_\infty^2c^2}{U_\infty^2}\ \phi_{tt} = 0 \qquad (1)$$

where θ is the angle the oncoming stream makes with the x-axis. The equation used by Nixon and Kerlick (References 8 and 10) is the classic, isolated airfoil equation

$$(1-M_\infty^2)\ \phi_{xx} + \phi_{yy} - 2\ \frac{c}{U_\infty}\ M_\infty^2\ \phi_{xt} - \frac{M_\infty^2\ c^2}{U_\infty^2}\ \phi_{tt} = 0 \qquad (2)$$

Hence, it can be seen that the Verdon and Caspar equations include the extra terms due to the y derivatives which are necessary to model highly curved blades. The boundary conditions for both equations are that there is no flow through a solid boundary. For the case of a flat plate at angle of attack α the boundary condition is

$$\phi_y(x,\pm\ 0) = -\ \alpha + \frac{c}{U_\infty}\ (x-x_o)\ \alpha_t \qquad (3)$$

where x_o is some pitching axis.

If θ is small, Equations (1) and (2) become identical. In the comparisons in Reference 10 θ is zero and, thus, the discrepancy reported cannot be due to the different equations. A possible cause of the discrepancy may be the different far field boundary conditions (see Section 3) but this has not been investigated.

3. FAR FIELD BOUNDARY CONDITIONS

The far field boundary condition used by Verdon and Caspar is that ϕ has the asymptotic form upstream of the cascade

$$\phi(x,y) = \sum_{j=-\infty}^{\infty} b_j \exp(iq_j y) \exp[(iM_\infty U_\infty \delta_j \pm d_j)(x-x_{-\infty})/\beta^2] \qquad (4)$$

where

$$q_j = (2\pi j+\sigma)/h, \quad \delta_j = M_\infty(\omega + U_\infty \sin\theta\, q_j)$$

$$\beta^2 = a_\infty^2 M_\infty^2 (1 - M_\infty^2 \cos^2\theta), \quad d_j^2 = (\beta^2 q_j^2 - \delta_j^2) M_\infty^2 a_\infty^2 \qquad (5)$$

and a_∞ is the speed of sound in the undisturbed flow, σ is the interblade phase angle and ω is the frequency of oscillation. $x_{-\infty}$ denotes the upstream computational boundary and h is the cascade gap.

The constant b_j is given by

$$b_j = h^{-1} \int_{\eta}^{\eta+h} \phi(\xi,\eta)\exp(-q_j\eta)d\eta \qquad (6)$$

Far upstream of the cascade a specified boundary condition is that the velocity components are given.

Thus as $x \to -\infty$

$$\phi(x,\eta) \to U_\infty \eta \sin\theta \qquad (7)$$

In the limit as $h \to \infty$, $q_j \to 0$ and, from equations (6) and (7)

$$b_j \to U_\infty \sin\theta \qquad (8)$$

In the study of asymptotic behavior there are two limits that can be examined as the gap approaches infinity. First, if the point $x_{-\infty}$ approaches $-\infty$ faster than $h \to \infty$ then the effect at $x_{-\infty}$ will always be that of a cascade. Second, if the point $x_{-\infty}$ does not

approach infinity faster than $h \to \infty$ then the behavior at $x_{-\infty}$ will be that of an isolated airfoil. Mathematically the first case is when

$$\lim_{\substack{x \to -\infty \\ h \to \infty}} \frac{x}{h} \neq 0 \tag{9}$$

while the second case is when

$$\lim_{\substack{x \to -\infty \\ h \to \infty}} \frac{x}{h} = 0 \tag{10}$$

In the case of an isolated airfoil the classic limit, on $y = 0$ as $x \to -\infty$, is (see, for example, Reference 15)

$$\phi(x,y) \to e^{iM_\infty^2 \Omega x} \frac{e^{iK|x|}}{(K|x|)^{1/2}} \tag{11}$$

where

$$\Omega = \nu/(1-M_\infty^2) \quad , \quad K = M_\infty \Omega \tag{12}$$

As $x \to -\infty$ the value of $\phi(x,y)$ given by Equation (11) decays as $|x|^{-1/2}$ whereas the form given by Equation (4) behaves as

$$\sum_{j=-1}^{1} U_\infty \sin\theta \exp\{i[M_\infty^2 \Omega \pm K](x - x_{-\infty})\} \tag{13}$$

and $b_j \to$ constant as $h \to \infty$. Note that as $h \to \infty$ the number of blade gaps must reduce to two with $j = \pm 1$ denoting the far field blades at $\eta = \pm \infty$.

Equation (13) does not give the isolated airfoil result as $h \to \infty$ if the limit of Equation (10) is imposed. It is suggested that this limit is the correct one to use for a far field computational boundary since $x_{-\infty}$ must be finite to be of any use.

4. STRONG SHOCK THEORY

In Reference 5 a modification to the unsteady high frequency small disturbance equation is described which alters the shock strength to give the Rankine Hugoniot value. These types of modifications improve the accuracy of the small disturbance equation. Reference 5 is attached as Appendix 1.

The theory of Reference 5 has been applied to the cascade code CTRAN. Since CTRAN and the base code XTRAN2L used in Reference 5 are similar the mechanics of coding the appropriate modifications proved to be easy. A detailed description of the modifications is given in Appendix 1. Typical results for a cascade are shown in Figures 1 and 2. The "strong shock" correction for a cascade is similar to that for isolated airfoil in that the shock waves are weakened and move forward. The section is a NACA0012; the amplitude is 1/4°, M_∞= 0.845 and h = 30. The large gap is used to indicate the effect of the modification. For more realistic values of the gap the strong shock modification may prove to be unnecessary because the shock waves in such conditions are relatively weak anyway unless the flow is nearly choked.

5. COMMENTS ON THE INDICIAL THEORY FOR CASCADE FLOWS

In Reference 1 a method of computing the unsteady flow through a cascade for any interblade phase angle using only one set of computational data is described. The computational data are calculated for a cascade with only one blade moving and the others held stationary. A further simplification is that only the indicial response for the cascade needs be computed; from this result the flow due to arbitrary time dependent motions can be constructed. In the previous report on the contract (Reference 10) attempts to compute the unsteady flow through

REFERENCES (Concluded)

9. Verdon, J. M. and Caspar, J. R.: Subsonic Flow Past an Oscillating Cascade with Finite Mean Flow Deflection. AIAA Journal, Vol. 18, No. 5, 1980.

10. Nixon, D.: Prediction Methods for the Unsteady Transonic Flow Through a Cascade. NEAR TR 306, 1983.

11. Steinhoff, J. S. and Jameson, A.: Multiple Solutions of the Transonic Potential Flow Equation. AIAA Journal Vol. 20, No. 11, 1982.

12. Salas, M. D., Gumbert, C. R., and Turkel, E.: Nonunique Solutions to the Transonic Potential Flow Equation. AIAA Journal, Vol. 22, No. 1, 1984.

13. Williams, M. H., Bland, S. R., Edwards, J. W.: Flow Instabilities in Transonic Small Disturbance Theory, NASA TM 86251, 1985.

14. Nixon, D.: Observations on the Occurrence of Multiple Solutions in Transonic Flow. NEAR Paper No. 179, 1985.

15. Nixon, D.: An Airfoil Oscillating at Low Frequencies in a High Subsonic Flow. British ARC CP 1285, 1974.

16. Nixon, D.: Perturbation of a Discontinuous Transonic Flow AIAA Journal, Vol. 16, No. 1, 1978.

REFERENCES

1. Nixon, D.: Computation of Unsteady Transonic Cascade Flows. AIAA Journal, Vol. 21, No. 5, 1983.

2. Nixon, D. and Klopfer, G. H.: Some Remarks on Transonic Potential Flow Theory. NEAR Paper 155, Journal of Applied Mechanics, Vol. 50, No. 2, 1983.

3. Nixon D.: Transonic Small Disturbance Theory with Strong Shock Waves. AIAA Journal, Vol. 18, No. 6, 1980.

4. Kerlick, G. D., Nixon, D., Ballhaus, W. F.: Unsteady Transonic Small Disturbance Theory with Strong Shock Waves. NEAR TR 230 (also AIAA Paper 82-0159), 1980.

5. Nixon, D.: Validation of a Computer Code to Treat Strong Shock Waves in a Transonic Flow. NEAR TR 316, 1983.

6. Ballhaus, W. F. and Goorjian, P. M.: Implicit Finite-Difference Computations of Unsteady Transonic Flows About Airfoils Including the Effect of Irregular Shock Motions. AIAA Journal, Vol. 15, No. 12, Dec. 1977.

7. Rizzetta, D. P. and Chin, W. C.: Effect of Frequency in Unsteady Transonic Flow. AIAA Journal, Vol. 17, No. 7, 1979.

8. Nixon, D. and Kerlick, G. D.: A High-Frequency Transonic Small Disturbance Code for Unsteady Flows in a Cascade. NEAR TR 277 (also AIAA Paper 82-0955), 1982.

$$\frac{(C_{L_\infty} - C_L)}{C_{L_\infty}} = \frac{A}{(h-h_o)^2} \qquad (60)$$

where C_{L_∞} is the value of C_L as $h \to \infty$, h_o is some value of h to be determined and A is a constant.

The computer code XTRAN2L, used for isolated airfoil problems, was modified to treat a steady cascade by the addition of periodic boundary conditions. A series of calculations for a NACA0012 cascade at $M_\infty = 0.845$ and $\alpha = 0$ was performed with various values of the gap, h. The results are shown in Figure 6.

If the value is h when C_L is zero (h = 22) and the value of C_L at h = 25 are used to compute h_o and A in Equation (60) then C_L can be computed. This value is also shown in Figure 4 and agrees very well with the computed results. This good agreement indicates that the compatibility equation, Equation (55), represents the behavior of nonunique solutions and that the general conclusions given in Appendix 2 apply to cascade flows.

6. CONCLUDING REMARKS

A number of points arising from previous work on cascade flows have been investigated and most have been clarified. There is still some question as to the correct far field boundary conditions to apply to unsteady cascade computations. However, the existence of nonunique solutions to the potential flow around cascade has been verified and examined.

If the gap is large the computationally effective flow field will be similar to that of an isolated airfoil since $\bar{u}$ and Δu will approach zero as $\eta \to \infty$. Consequently, the main contribution to the field integral will come only from values of u up to some distance $\tilde{h}$ from the blades. In other words

$$\int_o^h f(\eta)d\eta \simeq \int_o^{\tilde{h}} f(\eta)d\eta \tag{57}$$

where $\tilde{h}$ is independent of h. Consequently the field integrals in Equations (55) and (52) can be written, to a first approximation, as

$$\sum_{n=o}^{\infty} \int_{S_1} \int \bar{K}_{\xi x}^{(n)} [(g+I_f)^2 + (\frac{g}{g+I_f})^2] dS_1 \simeq \int_{\hat{S}_1} \int \bar{K}_{\xi x} [(g_1+I_{f_1})^2 + (\frac{g_1}{g_1+I_{f_1}})^2] d\hat{S}_1$$

$$+ \frac{1}{h^2} H_1(x,y) \tag{58}$$

and

$$I_f \simeq - \sum_{n=o}^{\infty} \frac{1}{4\pi} \int_{\hat{S}_1} \int \Delta K_{\xi x}^{(n)} f_1 d\hat{S}_1 + \frac{1}{h^2} H_2(x,y) \tag{59}$$

where $H_1(x,y)$ and $H_2(x,y)$ are independent of h and f_1 is similar to the eigensolution for the isolated airfoil. g_1 and I_{f_1} are associated with f_1. $\hat{S}_1$ is a subset of S_1 with a range $0 \leq \eta \leq \tilde{h}$ rather than $0 \leq \eta \leq h$.

By examining Equations (55), (58) and (59) it can be deduced that the compatibility equation, Equation (55), is similar to that of the isolated airfoil case, with the addition of a perturbation depending on the parameter $\frac{1}{h^2}$. From the general transonic perturbation theory of Reference 16 it is expected that the variation of C_L in a nonunique solution will vary as $\frac{1}{h^2}$.

If the perturbation parameter is of the form $\frac{1}{h^2}$ it follows that the lift coefficient for a cascade is of the form

If a function g(x,y) is defined as

$$g(x,y) = f_1(x,y) - \frac{f_1^{(o)}(x)}{1 - \bar{u}_o} \tag{50}$$

Then

$$\Delta u = g/(\bar{u}) \tag{51}$$

From Equations (42) and (50)

$$\left(\frac{1 - \bar{u}}{\bar{u}}\right) g = -\sum_{n=0}^{\infty} \frac{1}{4\pi} \int_{S_1} \int \Delta K_{\xi x}^{(n)} f_n dS_1 = I_f \tag{52}$$

Using Equations (51) and (52) then gives

$$\bar{u} = \frac{g}{g + I_f} \tag{53}$$

$$\Delta u = g + I_f \tag{54}$$

Substitution of Equations (53) and (54) into Equation (47) gives

$$\frac{g}{g+I_f} - \frac{1}{2}\left[\left(\frac{g}{I_f+g}\right)^2 + (g+I_f)^2\right] = \bar{u}_{T_L} - \sum_{n=o}^{\infty} \frac{1}{4\pi} \int_{S_1} \int \bar{K}_{\xi x}^{(n)} \left[(g+I_f)^2 + \left(\frac{g}{g+I_f}\right)^2\right] dS_1 \tag{55}$$

This equation must have a nonzero solution for f_n if a nonunique solution exists.

Consider now the case when the gap is large.

To a first approximation

$$\bar{u}_{T_L}(x,y) = \bar{u}_{T_L}^{(o)}(x,y) + \frac{1}{h^2} \bar{u}_{T_L}^{(1)}(x,y) \tag{56}$$

where $u_{T_L}^{(o)}$ is the value for the isolated airfoil and $u_{T_L}^{(1)}$ is a function independent of h.

$$f_n^{(o)} = \dot{f}_n\ (\xi,o)$$

An alternate form of Equation (42) is

$$F_{xx} + F_{yy} = \sum_{n=o}^{\infty} f_{n_x} \tag{44}$$

with the boundary condition

$$F_y(x,\pm nh) = 0, \tag{45}$$

where

$$F(x,y) = \int^x \frac{1}{\bar{u}(\xi,y)} \{f_1(\xi,y) - \frac{[1-\bar{u}(\xi,y)]}{[1-\bar{u}(\xi,o)]} f_1^{(o)}(\xi)\}d\xi$$

$$= \int^x \{\Delta u(\xi,y) - \Delta u(\xi,o)\}d\xi \tag{46}$$

Equation (44) and (46) are similar to Equation (44) and (46) in Reference 14 and the nonuniqueness analysis is then similar to that in Reference 14.

The symmetric part of Equation (37) is

$$\bar{u} - \frac{(\bar{u}^2 - \Delta u^2)}{2} = \bar{u}_{T_L} - \sum_{n=0}^{\infty} \frac{1}{4\pi} \int_{S_1} \bar{K}_{\xi x}^{(n)} (\bar{u}^2 + \Delta u^2) dS_1 \tag{47}$$

where

$$\bar{K}_{\xi x}^{(n)} = \frac{1}{2} [K_{\xi x}^{(n)}(x,y) + K_{\xi x}^{(n)}(\xi,-y)] \tag{48}$$

and

$$\bar{u}_{T_L}(x,y) = \sum_{n=-\infty}^{\infty} \frac{1}{2\pi} \int_o^1 \frac{\Delta v_o(x - \xi)}{[(x-\xi)^2 + (y-nh)^2]} d\xi \tag{49}$$

The asymmetric part of Equation (37) can be written as

$$\Delta u - \Delta u\bar{u} = \sum_{n=-\infty}^{\infty} \frac{1}{4\pi} \int_o^{\infty} \{ \frac{\Delta v_o(x-\xi)}{[(x-\xi)^2 + (y-nh)^2]} d\xi + \frac{1}{2\pi} \int_o^{\infty} \frac{\Delta u_o(y+nh)}{[(x-\xi)^2 + (y+nh)^2]} d\xi \}$$

$$- \sum_{n=0}^{\infty} \int_{S_1} \int [K_{\xi x}^{(n)}(x,y) - K_{\xi x}^{(n)}(x,-y)] \, \Delta u\bar{u} dS_1 \qquad (38)$$

From Equation (28) and (30)

$$\Delta u\bar{u} - (2n+1)\Delta u_o = f_n \qquad (39)$$

This equation specifies Δu in the flow field in terms of f_n. Since Equation (38) also specifies Δu in the flow field in terms of Δu_o there must be a compatibility relation.

Equation (38) can be written as

$$\Delta u - \Delta u\bar{u} = - \sum_{n=0}^{\infty} \frac{1}{4\pi} \int_{S_1} \int \Delta K_{\xi x}^{(n)} [\Delta u\bar{u} - (2n+1)\Delta u_o] dS_1 \qquad (40)$$

where

$$\Delta K_{\xi x}^{(n)} = [K_{\xi x}^{(n)}(x,y) - K_{\xi x}^{(n)}(x,-y)] \qquad (41)$$

Using Equation (39), Equation (40) can be written as

$$\frac{1}{\bar{u}} \{ f_1 - \frac{(1-\bar{u})}{(1-\bar{u}_o)} f_1^{(o)} \} = f_1 - \sum_{n=0}^{\infty} \frac{1}{4\pi} \int_{S_1} \int \Delta K_{\xi x}^{(n)} f_n dS_1 \qquad (42)$$

and

$$\Delta u_o = \frac{f_1^{(o)}}{\bar{u}_o - 1}$$

$$\Delta u = \frac{1}{\bar{u}} \{ f_1 + \frac{f_1^{(o)}}{(\bar{u}_o - 1)}] \qquad (43)$$

where

$L(\bar{v}_o)$ is an integral operator on $\bar{v}_o$

such that

$$-\frac{1}{2\pi}\sum_{n=-\infty}^{\infty}\int_0^1 \frac{L(\bar{v}_o)(x-\xi)}{[(x-\xi)^2+n^2h^2]}d\xi = \bar{v}_o \tag{33}$$

The fact that a lifting solution to the linear problem exists such that

$$\Delta u_o = L(\bar{v}_o) \tag{34}$$

is significant evidence that $L(\bar{v}_o)$ exists.

Equation (32) can be written in the form

$$0 = -\sum_{n=0}^{\infty}\int_{S_1}\int K^{(n)}_{\xi y_o}\{\Delta u(\xi,\eta)\bar{u}(\xi,\eta) - (2u+1)[\Delta u_o - L(\bar{v})]\}dS_1 \tag{35}$$

Equation (44) is similar to Equation (30) and indicates that a nonzero function, f_n, exists, which satisfies Equation (30), and is given by

$$f_n = \Delta u(\xi,\eta)\bar{u}(\xi,\eta) - (2u+1)[\Delta u_o - L(\bar{v}_o)] \tag{36}$$

where the right-hand side is generated from a real transonic solution.

Now differentiate Equation (21) with respect to x, giving

$$u - \frac{u^2}{2} = \sum_{n=-\infty}^{\infty}\{\frac{1}{2\pi}\int_0^{\infty}\frac{\Delta v_o(x-\xi)}{[(x-\xi)^2+(y-nh)^2]}d\xi + \frac{1}{2\pi}\int_0^{\infty}\frac{\Delta u_o(y-nh)}{[(x-\xi)^2+(y-nh)^2]}d\xi\}$$

$$-\frac{1}{2}\int_S\int K_{\xi x}u^2 dS \tag{37}$$

where

$$\bar{v}(x,o) = \frac{1}{2}\,[v(x,+o) + v(x-0)] \tag{26}$$

and it has been noted that, because of periodicity,

$$\Delta u(\xi,nh) = \Delta u(\xi,o) = \Delta u_o \tag{27}$$

The subscript o denotes a value on y = 0. Equation (25) can be written as

$$\bar{v}(x,o) = -\sum_{n=o}^{\infty} \int_{S_1} \int K_{\xi y_o}^{(n)}\,[\Delta u(\xi,\eta)\bar{u}(\xi,\eta) - (2n+1)\Delta u_o]\,dS_1 \tag{28}$$

where S_1 now covers one blade gap

$$K^{(n)} = \frac{1}{4\pi}\ln[(x-\xi)^2 + (\eta-nh-y)^2] \tag{29}$$

Equation (28) is similar to one in Reference 14 and for a lifting solution to exist when

$$\bar{v}(x,o) = 0$$

a function, f_n, must exist such that

$$-\sum_{n=o}^{\infty} \int_{S_1} \int K_{\xi y}^{(n)} f_n\,dS_1 = 0 \tag{30}$$

and

$$f_n \neq 0 \tag{31}$$

In order to establish the existence of f_n it is necessary to write Equation (25) as

$$0 = \sum_{n=-\infty}^{\infty} \{\frac{1}{2\pi} \int_o^{\infty} \frac{[\Delta u_o - L(v_o)]\ (x-\xi)}{[(x-\xi)^2 + n^2h^2]}\,d\xi\} - \frac{1}{2\pi}\int_S \int K_{\xi y_o} u^2\,dS \tag{32}$$

Analysis of Nonunique Solutions

A cascade is composed of an infinite number of blades or airfoils and an integral representation of the TSD equation can be constructed in a similar way as that for an isolated airfoil (described in Reference 14) using the principle of superposition. Thus,

$$\phi(x,y) = \sum_{n=-\infty}^{\infty} \{\int_o^{\infty} [\Delta v K_o^{(n)} - \Delta\phi K_{\eta_o}^{(n)}]\, d\xi\} - 1/2 \int_S \int K_\xi u^2 dS \qquad (21)$$

where

$$K_o^{(n)} = \frac{1}{4\pi} \ell n \left| (x-\xi)^2 + (nh-y)^2 \right| \qquad (22)$$

and

$$K = \frac{1}{4\pi} \ell n \left| (x-\xi)^2 + (y-\eta)^2 \right| \qquad (23)$$

Differentiation of Equation (21) with respect to y gives

$$v(x,y) = \sum_{n=-\infty}^{\infty} \{\int_o^{\infty} \frac{\Delta v(\xi,nh)(y-nh)}{[(x-\xi)^2 + (y-nh)^2]}\, d\xi - \int_o^{\infty} \frac{\Delta u(\xi,nh)\,(x-\xi)}{[(x-\xi)^2 + (y-nh)^2]}\, d\xi\}$$
$$- \frac{1}{2} \int_S \int K_{\xi y} u^2 dS$$

The operator "Δ" is defined as

$$\Delta f(x,y) = \frac{1}{2} [f(x,+y) - f(x-y)] \,. \qquad (24)$$

On $y = 0$ the first sum yields the value $\frac{\Delta v}{2}$; note that since $\Delta v(\xi,\eta)$ is periodic about each blade the terms for $n = \pm N$ cancel. Equation (24) can thus be written as

$$\bar{v}(x,o) = - \sum_{n=-\infty}^{\infty} \frac{1}{2\pi} \int_o^{\infty} \frac{\Delta u(\xi,o)(x-\xi)}{[(x-\xi)^2 + n^2h^2]} d\xi - \frac{1}{2} \int_S \int K_{\xi y_o} u^2 dS \qquad (25)$$

addition to the cascade result, results for both a free air and for a solid wall boundary condition are shown; in these cases the far field boundary is at the same location as for the cascade result. It can be seen that the behavior with the various boundary conditions is different even though the boundary is at a nominally far field location. The behavior of a nonunique solution with decreasing gap is shown in Figure 6 and is compared with the result for a solid wall boundary condition. The difference is quite significant. It also appears that the cascade effect inhibits the appearance of the nonuniqe solution since it does not appear for practical gap/chord ratios for this particular section.

The cascade code was used to investigate the behavior of the nonunique solutions in oscillatory flows. These oscillatory solutions were started from either a zero lift condition or a nonunique steady state. The results are shown in Figure 7; and it can be seen that the oscillatory perturbation is nearly sinusoidal but is about a non zero lift. The section is the NACA0012, $M_\infty = 0.845$, the pitch amplitude is 1/4° and the reduced frequency is 1.0. It is also noted that the solution starting from a zero lift condition is not converged but appears to be approaching the other results. As a final result the cascade code with the strong shock conditions was run for the same case and the results seem to be of the unique variety. The steady state solution is symmetric in this case in order to provide symmetric controls for the strong shock addition; asymmetry is introduced by allowing a non zero mean angle of attack for the first 200 time steps.

It is desirable to examine the behavior of these nonunique solutions and this is done in the next section.

$\bar{C}_L$ will be infinite. For the flat plate reported case by Verdon and Caspar with $M_\infty = 0.5$, $h = 1$, $\nu = 1$ Equation (20) gives, for $p = 0$,

$$\sigma = \pm 33.1°$$

which is the interblade phase angle for resonance found by Verdon and Caspar.

Results for the flat plate case, computed using Equation (24) and 100 blades, are shown in Figure 3. In this calculation the total number of blades in the numerical computation is 13 and $m = 3$. A transonic case for a NACA0012 section, $M_\infty = 0.75$, $h = 2.0$ is shown in Figure 4.

Nonunique Solutions

Over the last six years nonunique solutions to the transonic potential equation have been found. (See References 11 and 12). In the initial cases these consisted of lifting solutions for the flow around symmetric airfoils at zero angle of attack. Later, nonunique solutions were found for nominally lifting conditions. These nonunique solutions have been found for isolated airfoils and for airfoils in wind tunnels; unsteady solutions have also been reported in Reference 13. In the present work, nonunique solutions have been found for cascade solutions.

In order to find the nonunique solutions the cascade code, CTRAN, developed under previous work on the contract, was used. Also, a variant of the code XTRAN2L, modified to give periodic boundary conditions, was used. Only steady flows are considered at the moment. For a gap of 50 chord lengths the range of Mach numbers for a nonunique solution are shown in Figure 5. In

15). The lift induced on a blade is proportional to the induced upwash parameter, which is given by Equation (16). Hence it follows that

$$C_{L_n} = C_{L_m} \left|\frac{m}{n}\right|^{1/2} e^{iK(|n|-m)\bar{h}} \tag{17}$$

where the relation $\bar{y} = n\bar{h}$ is used, and m is a given blade beyond which Equation (16) is a good approximation. It is assumed that C_{L_m} is known. Note that the actual value of v(x,y) is not given by Equation (16) since this result only holds if there are no other blades. However, the actual upwash will vary with y in a form similar to Equation (16). Using Equations (14), (15) and (24) gives

$$\tilde{C}_L = \sum_{n=-m+1}^{m-1} \tilde{C}_{L_n} e^{-in\sigma} + \sum_{n=m}^{\infty} \tilde{C}_{L_m} \left(\frac{m}{n}\right)^{1/2} \exp[iK(n-m)\bar{h}-in\sigma]$$

$$+ \sum_{n=-\infty}^{-m} \tilde{C}_{L_{-m}} \left(\frac{m}{n}\right)^{1/2} \exp[-iK(n+m)\bar{h}-in\sigma] \tag{18}$$

It can be seen that the effect of the cascade blades diminishes as $n^{-1/2}$ and hence a large number of blades is necessary in the initial computation of C_{L_n} unless the approximation of Equation (17) is used. It is also of interest to examine further Equation (18). The two infinite sums are bounded (see Appendix 4) unless

$$\pm K\bar{h} - \sigma = 2p\pi \tag{19}$$

where p is an integer. Thus for an interblade phase angle, given by

$$\sigma = \pm K\bar{h} - 2p\pi \tag{20}$$

cascades are described. The results did not agree very well with those of Verdon and Caspar (Reference 9) and hence, some examination into the causes of the discrepancy is necessary.

In Reference 10 the computed data are for a seven blade cascade and it is possible that this restricted number of blades is a cause of the discrepancy. This aspect is elaborated below.

The lift given by the theory in Reference 1 is

$$C_L(t) = \sum_{n=-\infty}^{\infty} C_{L_n}(t - n\,\sigma) \tag{14}$$

where C_{L_n} is the lift induced at blade zero by the motion of the n^{th} blade with the other blades stationary and σ the interblade phase angle.

If the flow is harmonic in time,

$$\begin{aligned} C_L(t) &= \tilde{C}_L e^{i\omega t} \\ C_{L_n}(t - n\sigma) &= \tilde{C}_{L_n} e^{i\omega(t - n\sigma)} \end{aligned} \tag{15}$$

In a cascade the unsteady flow induced on blade zero by the n^{th} blade can be characterized by the asymptotic form of the unsteady flow provided the n^{th} blade is sufficiently far from blade zero (for example several chord lengths). The asymptotic behavior for the induced normal velocity is (Appendix 3)

$$v(x,y) \tilde{\sim} A \frac{e^{iK|\bar{y}|}}{(K|\bar{y}|^{1/2})}, \tag{16}$$

where A is a complex constant and $\bar{y} = (1-M_\infty^2)^{1/2} y$. This result is obtained from classic subsonic airfoil theory (see Reference

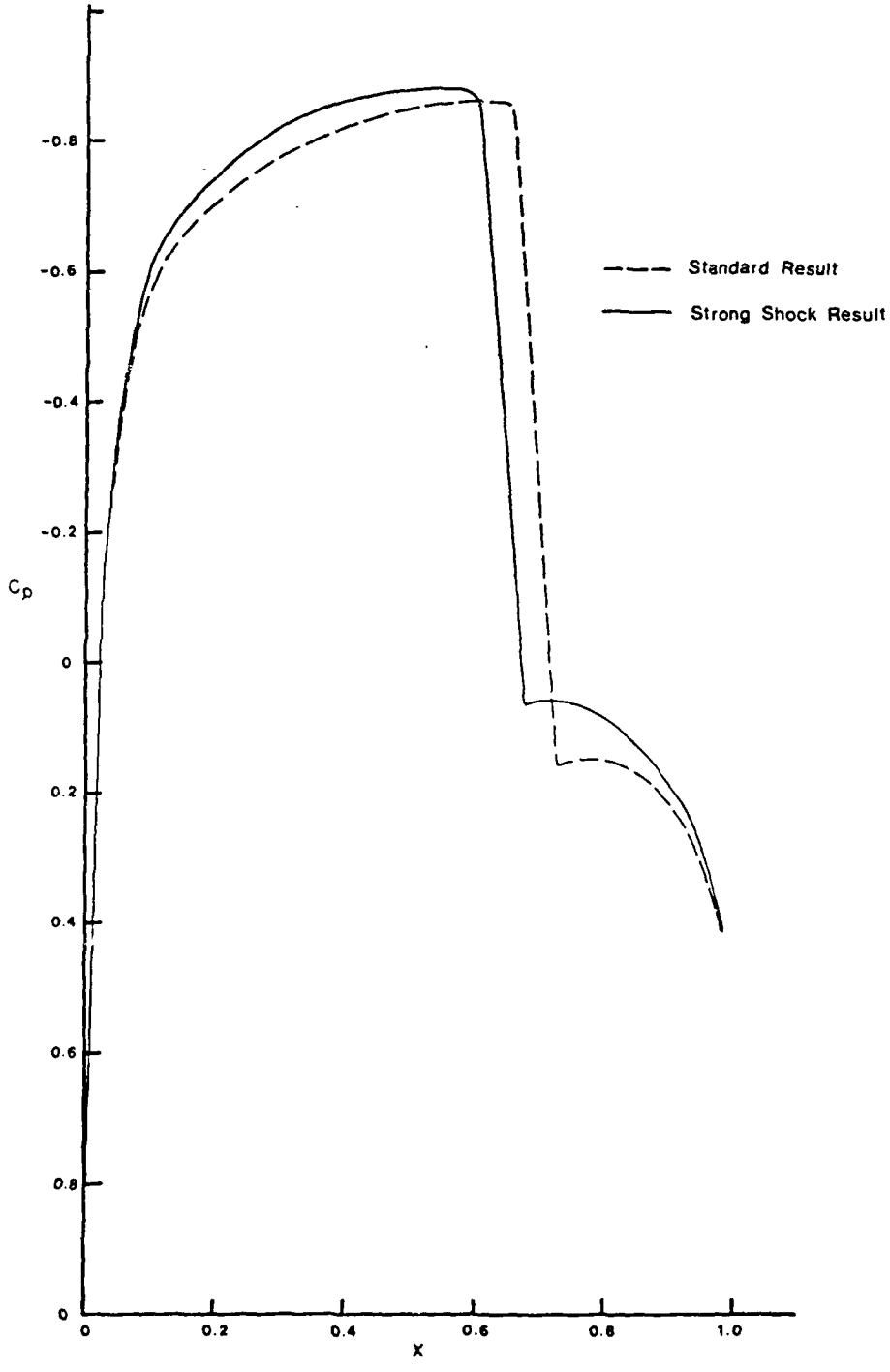

Steady pressure distribution through a cascade $M_\infty = 0.845$, $\alpha = 0$, $h = 30$.

Figure 1

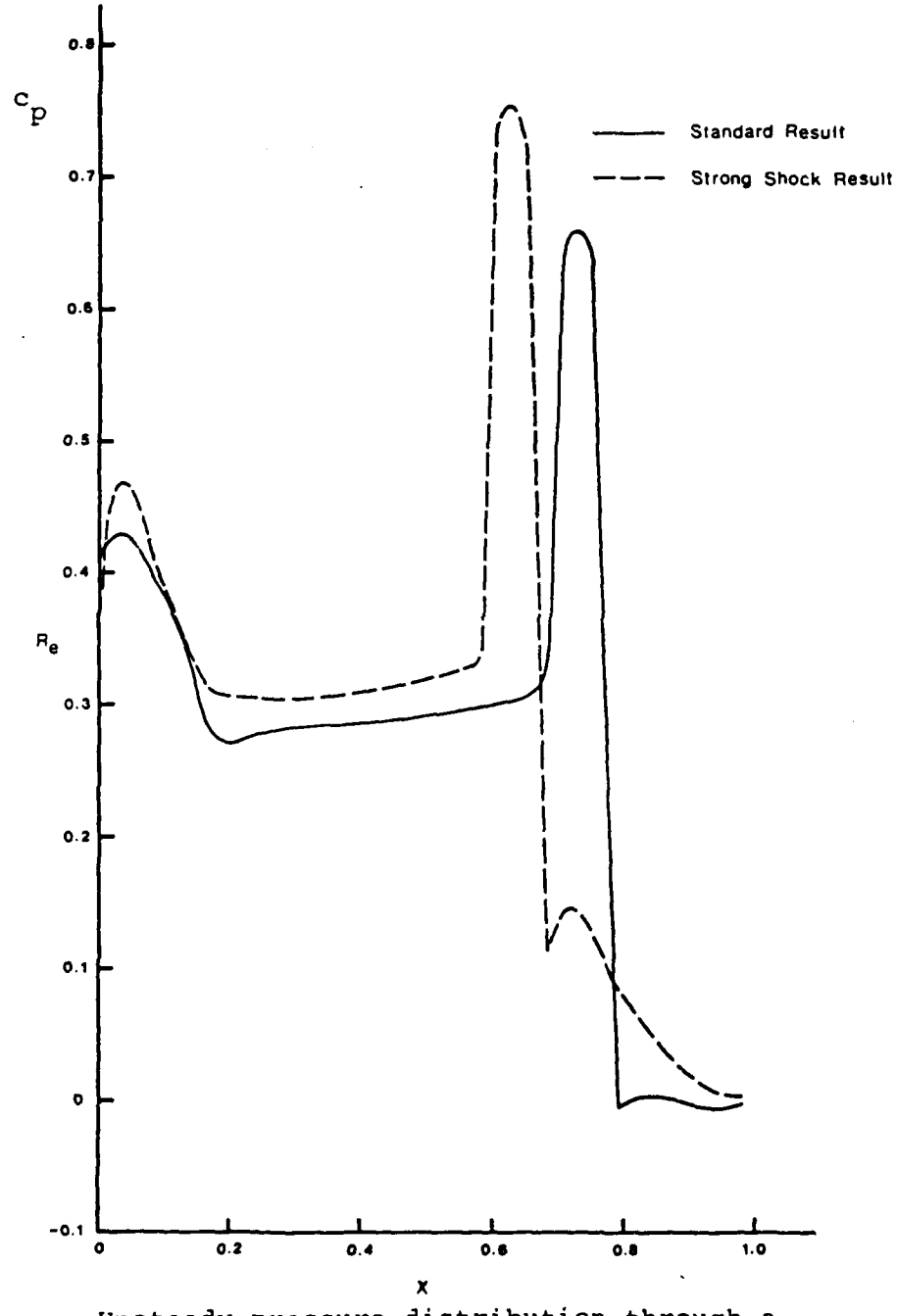

Unsteady pressure distribution through a cascade $M_\infty = 0.845$, $\alpha_1 = 0.25°$, $h = 30$.

Figure 2a

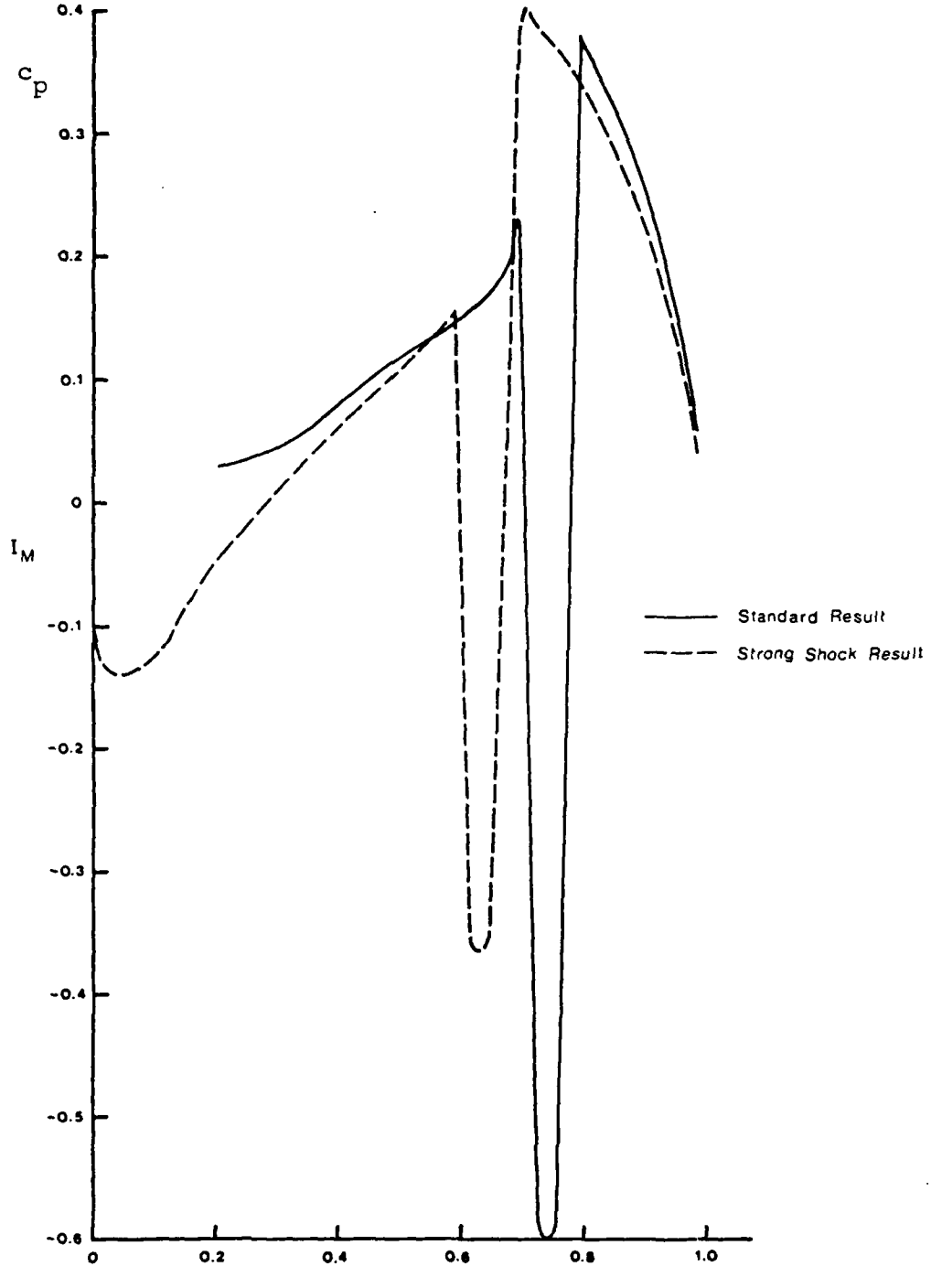
0.4
c_p
0.3
0.2
0.1
0
I_M
-0.1
-0.2
-0.3
-0.4
-0.5
-0.6
0
0.2
0.4
0.6
0.8
1.0
Standard Result
Strong Shock Result

Figure 2b

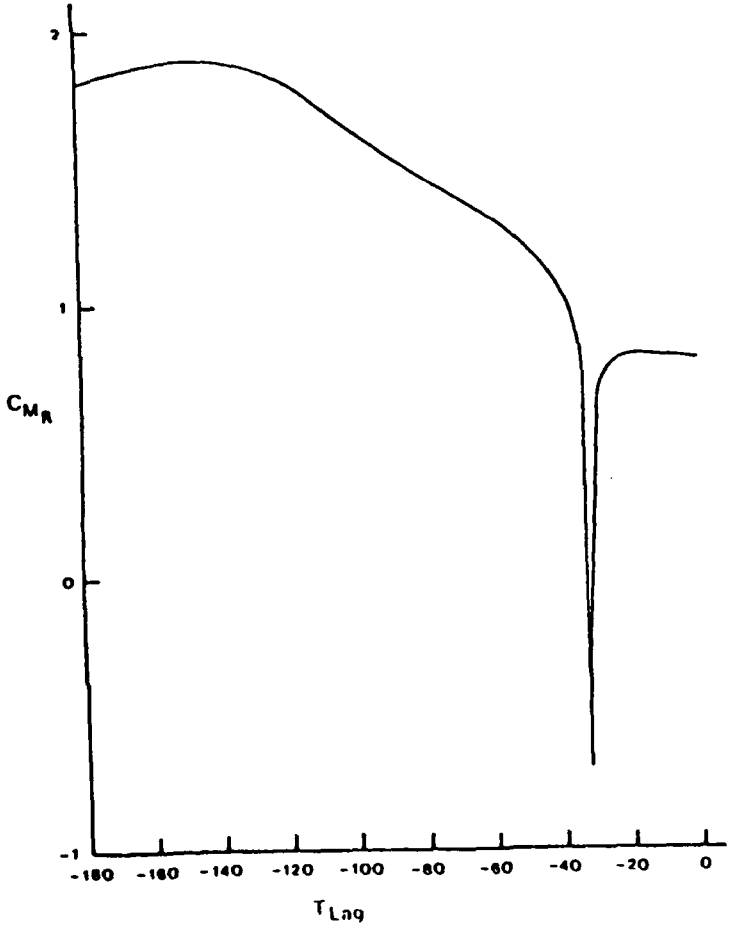

(a)

Moment due to torsion for a flat plate; $M_\infty = 0.5$, $\nu = 1.0$, $h = 1.0$.

Figure 3

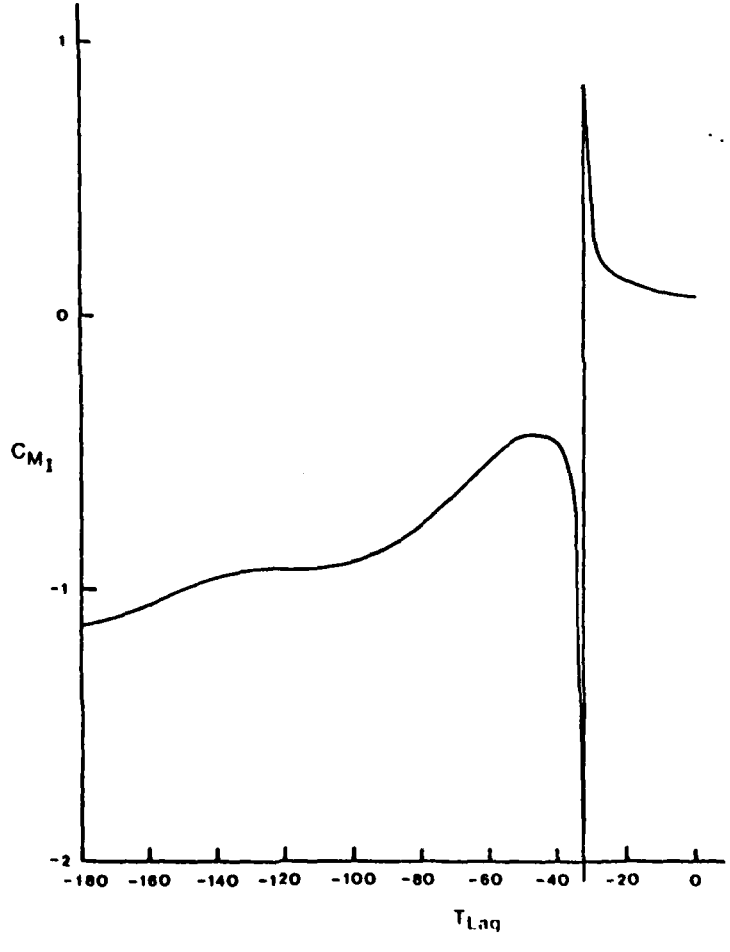

(b)

Figure 3

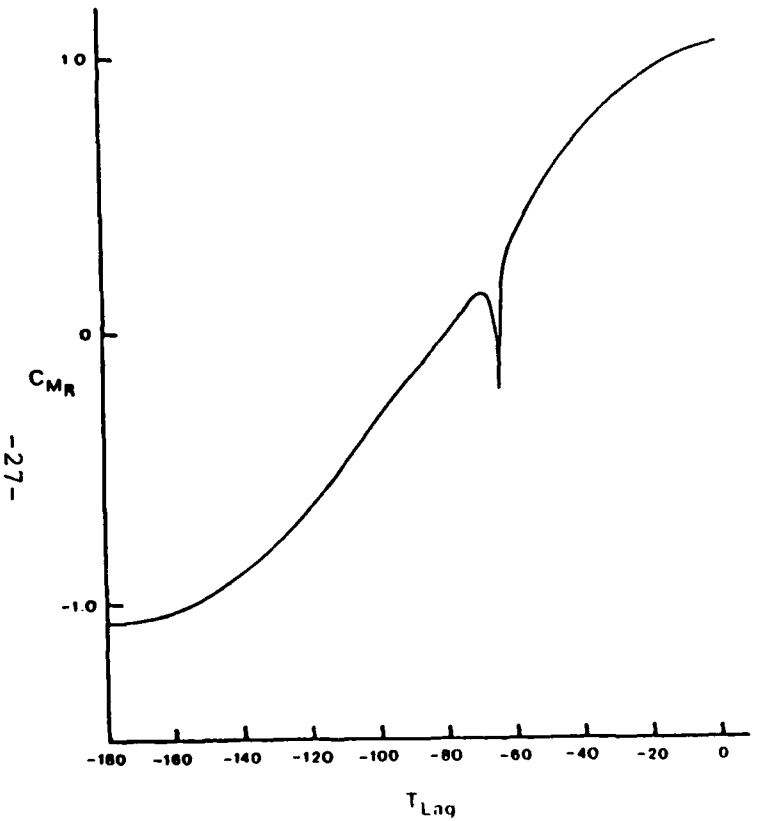

(a)

Moment due to torsion for a NACA0012 section: $M_\infty = 0.75$, $\nu = 1.0$, $h = 2$.

Figure 4

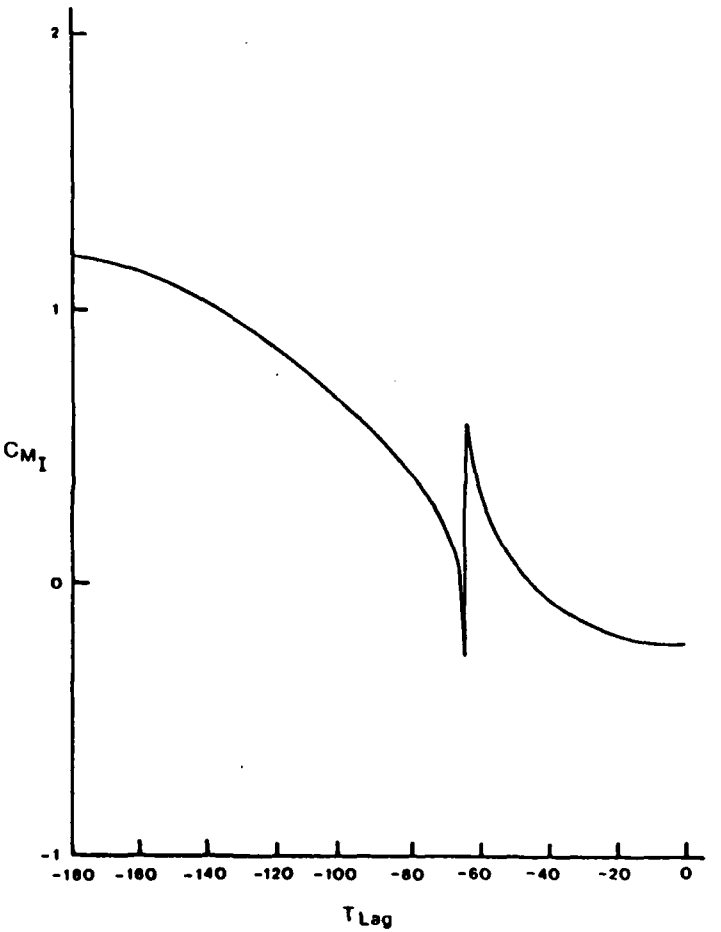

(b)

Figure 4

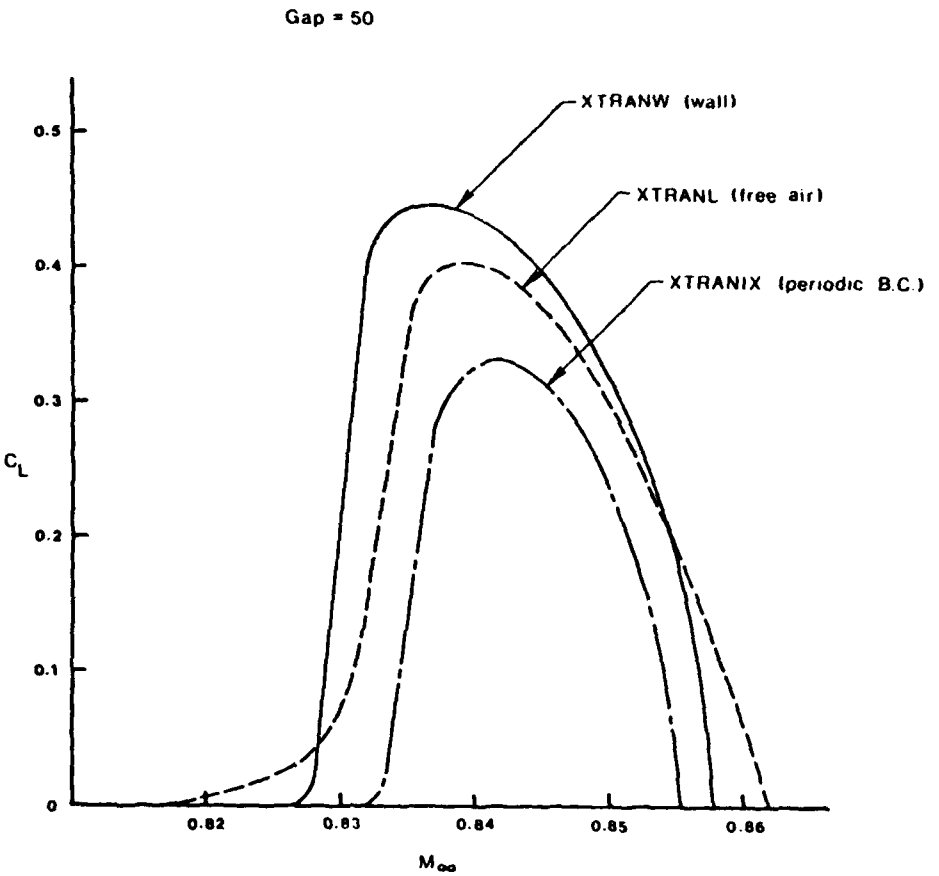

Variation of nonunique behavior with Mach number.

Figure 5

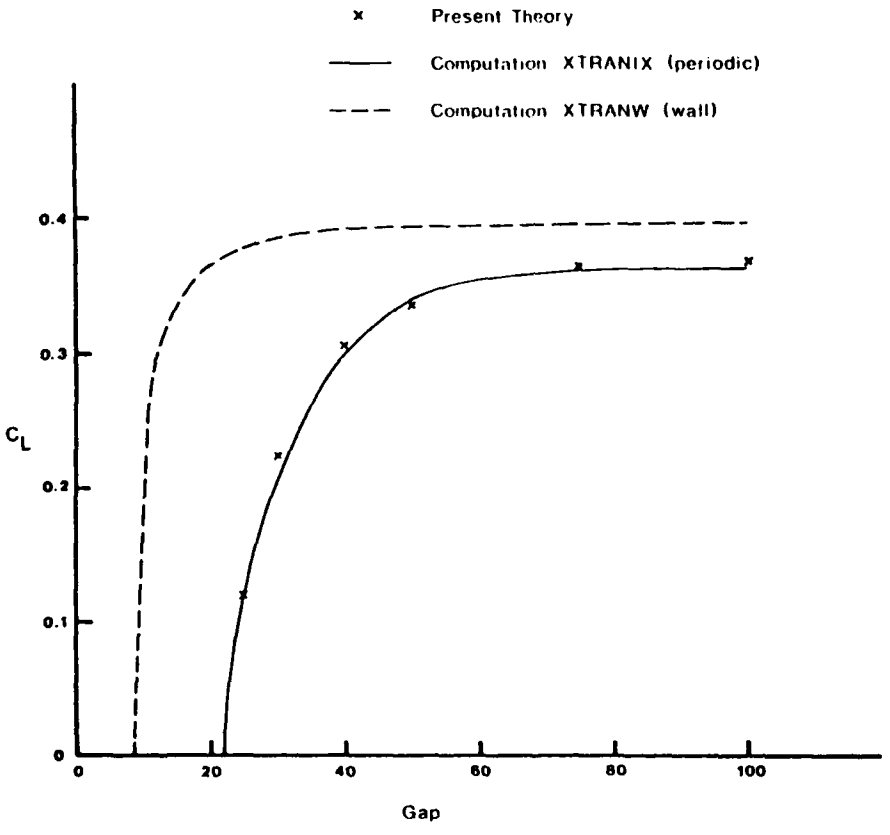

Variation of nonunique behavior with gap.

Figure 6

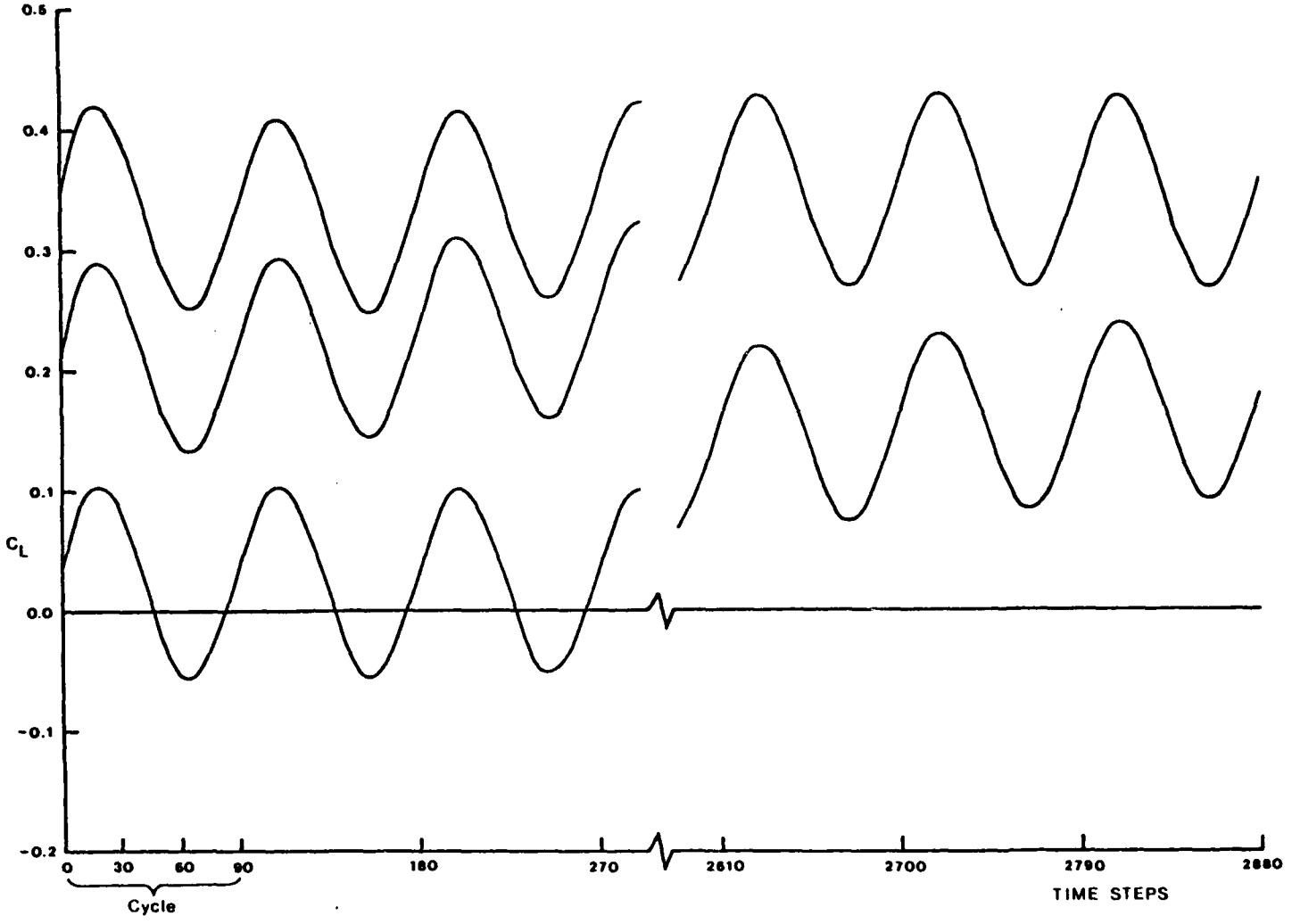

Unsteady nonunique behavior

Figure 7

APPENDIX 1

VALIDATION OF A COMPUTER CODE TO TREAT STRONG SHOCK WAVES IN A TRANSONIC FLOW

by

David Nixon

NEAR TR 316

December 1983

Prepared Under Contract NAS1-17316

for

NATIONAL AERONAUTICS AND SPACE ADMINISTRATION
Langley Research Center
Hampton, VA 23665

by

NIELSEN ENGINEERING & RESEARCH, INC.
510 Clyde Avenue, Mountain View, CA 94043
Telephone (415) 968-9457

TABLE OF CONTENTS

1. INTRODUCTION

The most common methods of predicting steady flow aerodynamic characteristics at transonic speeds are either the Transonic Small Disturbance (TSD) theory (Ref. 1) or the Full Potential Equation (FPE) theory (Ref. 2). The more accurate Euler equations solutions (Ref. 3) are expensive to obtain, although for flows with strong shock waves such solutions are essential. The FPE theory is based on the assumption that the flow is isentropic and irrotational and generally has a (numerically) exact treatment of wing boundary conditions. The TSD theory is an approximation to the FPE theory and thin wing boundary conditions are used in the solution procedure. One of the advantages of the TSD theory is the flexibility in deriving the approximate equation. This flexibility is generally utilized by a choice of a transonic scale parameter.

The basic assumptions of isentropy and irrotationality in both these theories are only valid when there are no shock waves (Ref. 4) in the flow. Although the potential theory is valid strictly only for shock-free flows, the results obtained by such a theory for flows with shock waves are sufficiently close to experimental data for practical use, provided the shock waves are weak. The generally accepted definition of a weak shock is when the local Mach number just ahead of the shock is less than 1.3. Thus, when both TSD and FPE solutions are compared to the more realistic Euler equation solutions it is found that the agreement is satisfactory provided that the basic restriction to weak shock waves is not violated. The use of thin wing boundary conditions can also introduce errors into the TSD solutions.

If the flow has strong shock waves, however, then there is considerable disagreement between both TSD and FPE solutions and Euler equations solutions. Generally the predicted shock location for the potential theories is much further aft than that for the Euler equation solutions. The causes of the error in the shock location in the steady TSD theory for two-dimensional flow have been examined in Reference 4 where the basic justification for a correction procedure has been derived. The basic hypothesis of the theory is that the error in shock location is primarily due to the stronger shock predicted by TSD theory compared to the shock strength of the Euler equations. It is also assumed that if the shock strength is suitably corrected then the shock location should be approximately correct. These correction theories have been applied to both steady (Ref. 5) and unsteady (Ref. 6) solutions of the TSD equation and to the steady FPE.

The commonly used potential theories are based on Crocco's theorem which states that if the entropy gradient in the flow is negligible then an inviscid flow exists with negligible vorticity and hence a velocity potential derived under the assumption of zero vorticity gives a good approximation to the flow. However, application of Crocco's therem requires that mass, momentum and energy be conserved and since in a potential solution with shock waves momentum is not conserved, it can be seen that the transonic potential theory is not consistent with its basic assumptions. However, since transonic potential theory does give good results for flows with weak shock waves its use can be justified on the basis of practicability alone. A more flexible criteria for developing consistent theories is to introduce (Ref. 4) the idea of minimizing a weighted combination of source errors at the shock wave. For example, if mass and energy are conserved through a shock then the conventional potential theory results, or, if a suitable weighted sum of the mass, momentum, and energy errors are put to zero then a

potential equation with a specified shock jump results. Thus, a potential theory with a Rankine-Hugoniot shock jump can be obtained.

In Reference 5 the correction to the TSD equation is obtained by computing two steady state solutions and then using an interpolation technique to give the required solution. This technique is not really feasible for unsteady flow since the correction procedure is required for each time step in the two TSD solutions, with different scaling parameters, and an interpolation scheme derived for discontinous transonic flows. Examples of steady flows with strong shocks computed with this method agree satisfactorily with the Euler equation solutions, although the use of the thin airfoil boundary conditions in the TSD theory can give rise to errors near the leading edge.

An extension of the basic correction procedure for unsteady transonic flow is given in Reference 6 where the low frequency theory of Ballhaus and Goorjian (Ref. 8) is extended by adding a formally negligible third order term to the theory. The improvement in the potential theory for flows with strong shock waves is remarkable. The conventional theory failed to give an answer. However, this theory still has some problems, in particular, the agreement of the pressure distributions with the results of the Euler equations is unsatisfactory ahead of the shock wave. This is attributed to the global nature of the strong shock correction affecting the flow ahead of the shock wave as well as weakening the conventional potential shock.

Although all of the above theories have been vindicated by computations the number of examples computed is very small. Before any of these theories can be used in practice with some confidence a much more detailed validation is required.

In the present work, therefore, the application of the strong shock theory to unsteady flows will be tested in much greater detail than has been done at present.

In the present study it is found that the pressure error in the previous study is due to one of the additional parameters being unconstrained. Also, it has been found that the theory of Reference 7 is not easily extended to unsteady flows (see the Appendix). The theory is extended to treat high frequency flows. The results of the modified theory show a marked improvement over the earlier work of Reference 6.

2. BASIC EQUATIONS

The basic differential equation used in the present analysis is

$$(a + b\phi_x + c\phi_x^2)\phi_{xx} + \phi_{yy} + A\phi_{xt} + B\phi_{tt} = 0 \tag{1}$$

where a, b, c are parameters to be chosen,

$$A = -2M_\infty^2 \nu/\delta^{2/3} \qquad B = -M_\infty^2 \nu^2/\delta^{2/3} \tag{2}$$

where M_∞ is the free-stream Mach number and ν is the reduced frequency. If δ is the airfoil thickness parameter, c is the airfoil chord and U_∞ the free-stream velocity, then x,y,t,ϕ are normalized with respect to c, $c/\delta^{1/3}$, ω^{-1}, $c\delta^{2/3}U_\infty$ where ω is the oscillation frequency.

The high frequency boundary condition is

$$\phi_y(x,\pm 0,t) = \frac{\partial f}{\partial x}(x,\pm 0,t) + \frac{\nu \partial f}{\partial t}(x,\pm 0,t) \tag{3}$$

where $y = f(x,\pm 0,t)$ denotes the upper and lower surfaces of the airfoil in motion, respectively. The far field boundary condition is a nonreflective boundary condition of the type developed by Kwak (Ref. 9) and is further developed by Whitlow (Ref. 10).

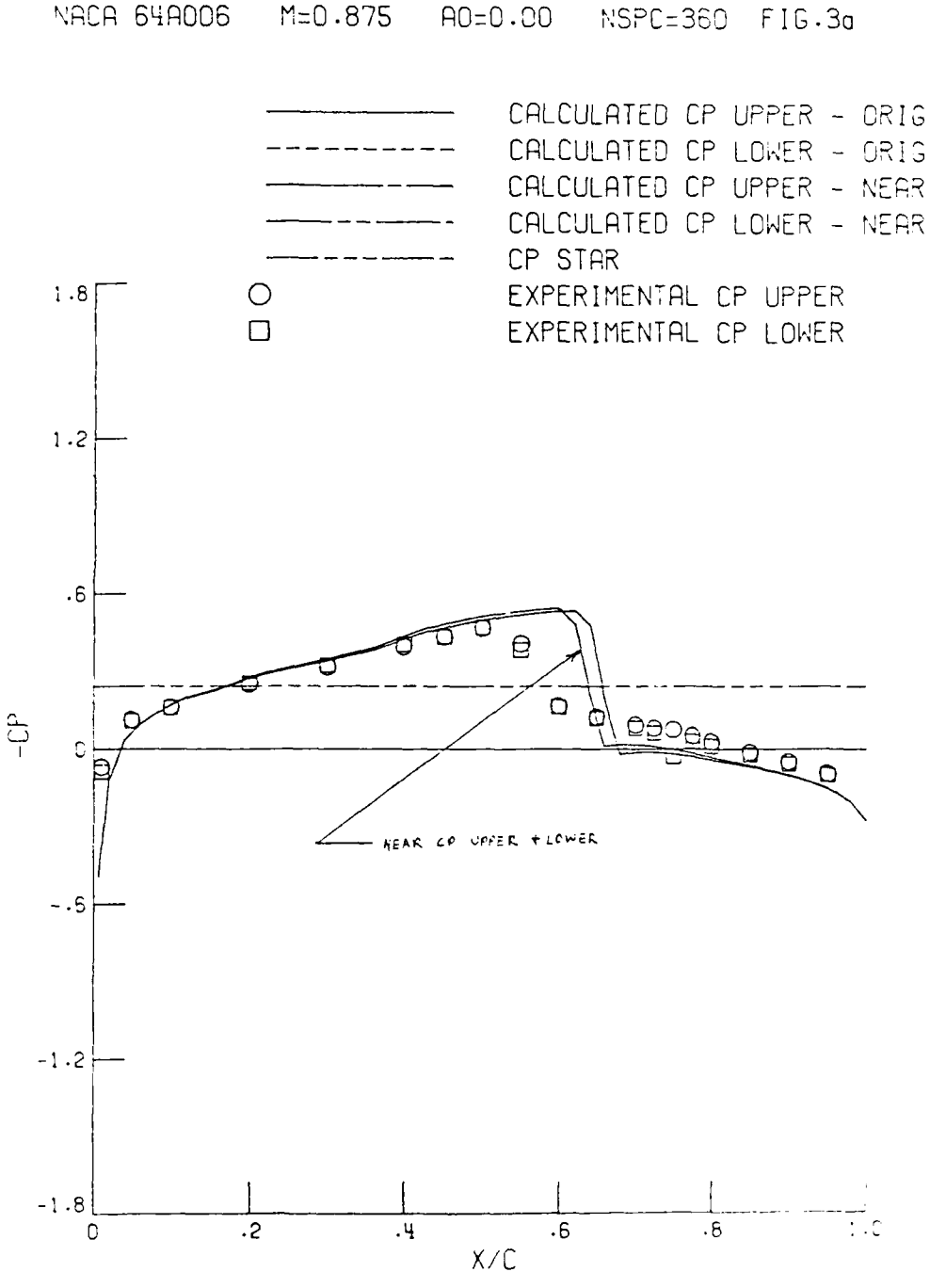

(a) Steady flow, $\alpha_0 = 0.0$

Figure 3.- Pressure distributions around a NACA 64A006 airfoil, $M_\infty = 0.875$.

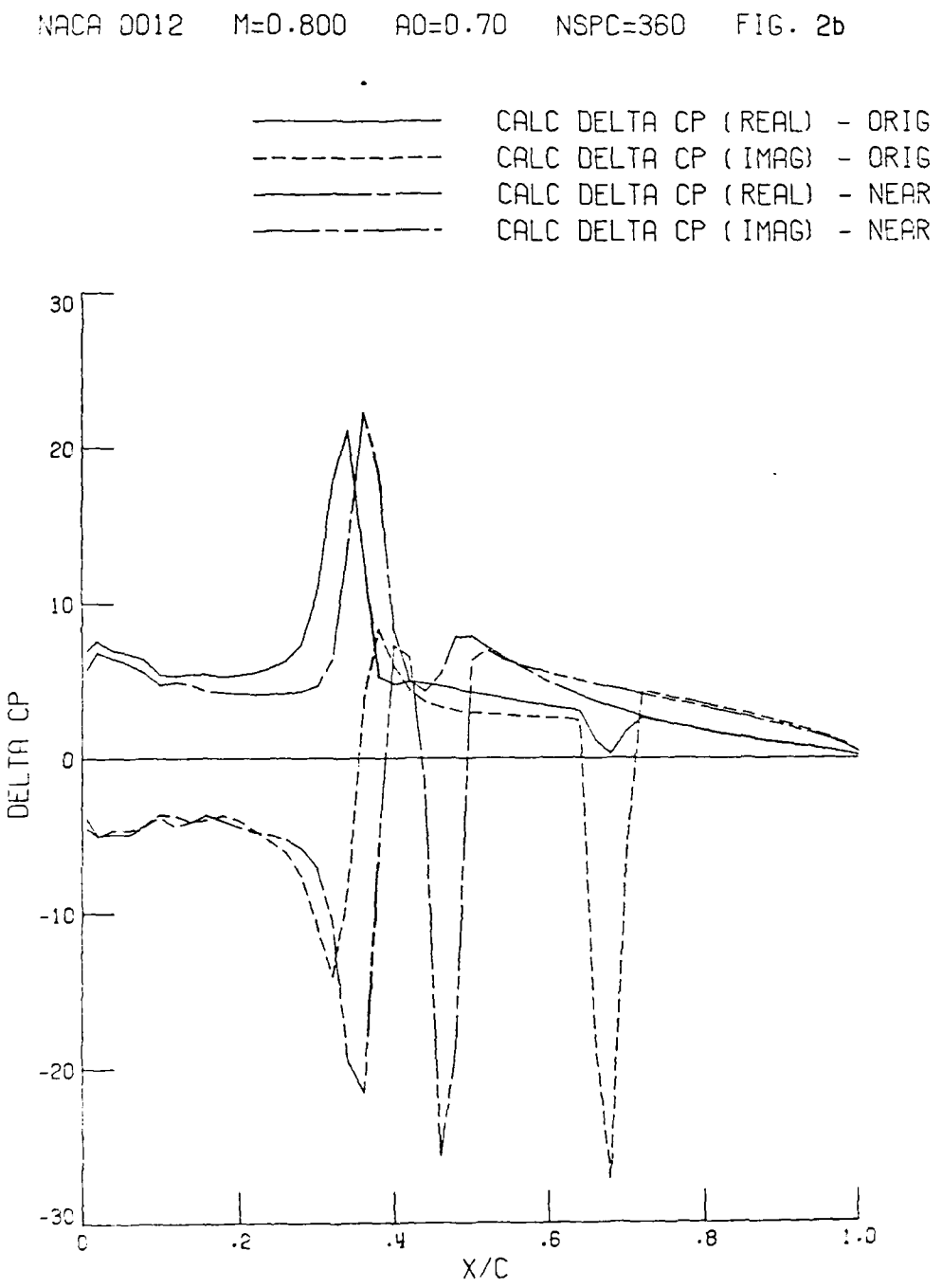

(b) Unsteady flow, $\alpha_1 = 0.25°$

Figure 2.- Concluded.

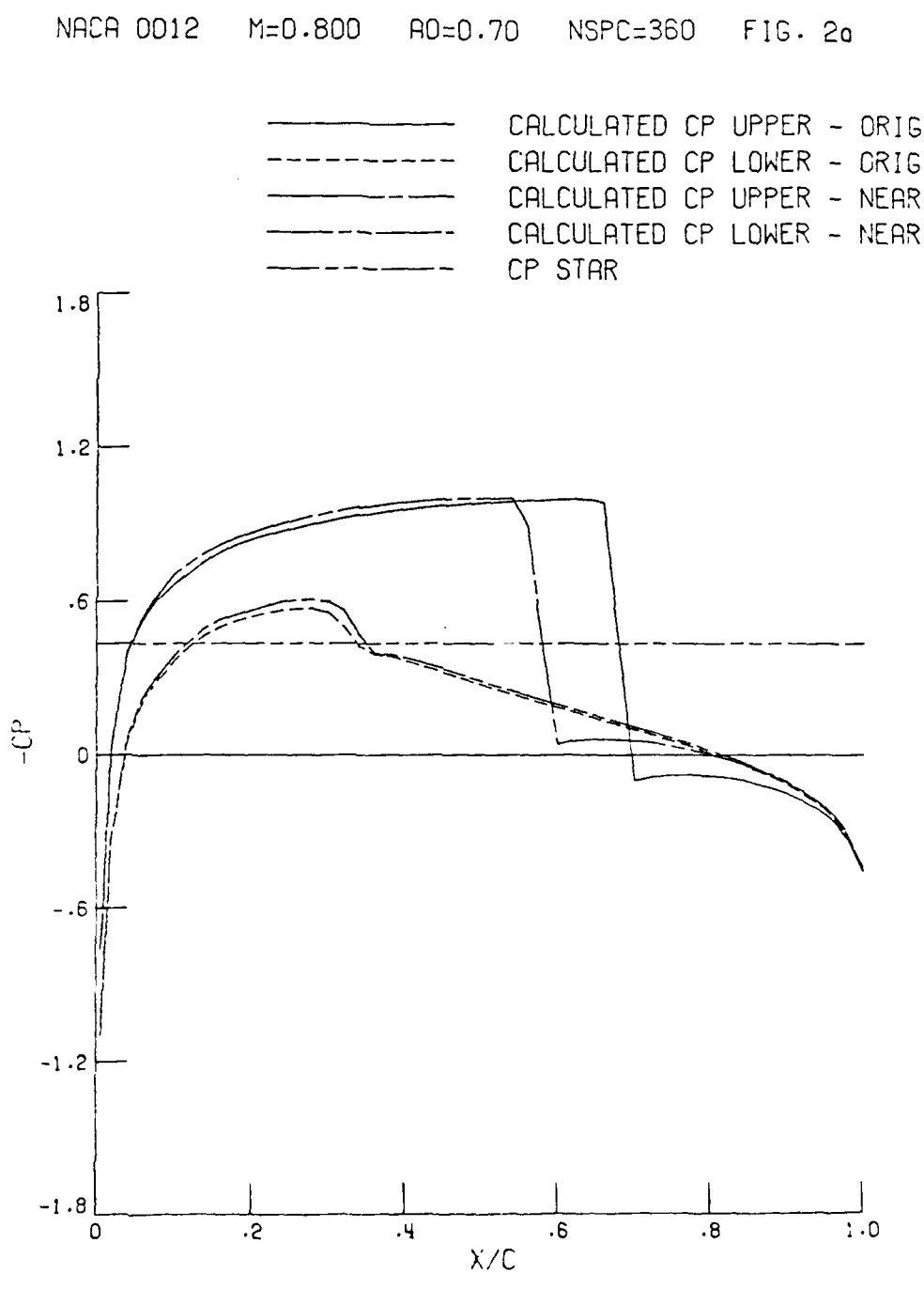

(a) Steady flow, $\alpha_0 = 0.7°$

Figure 2.- Pressure distributions around a NACA 0012 airfoil, $M_\infty = 0.8$.

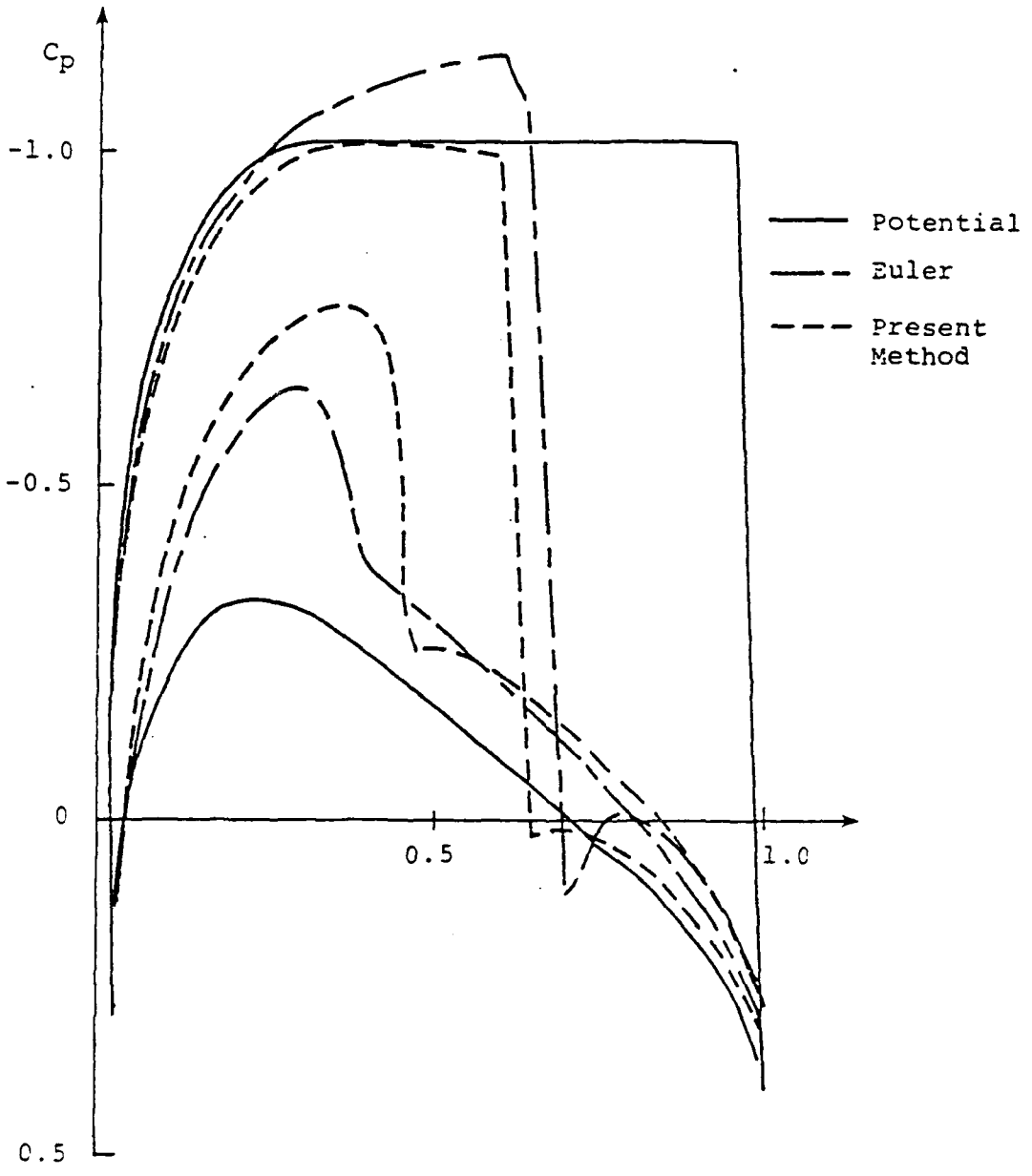

Figure 1.- Pressure distribution around a NACA 0012 airfoil, M_∞ = 0.8, α = 1.25°.

REFERENCES

1. Murman, E. and Krupp, J. A.: Computation of Transonic Flows Past Lifting Airfoils and Slender Bodies. AIAA Jour., Vol. 10, No. 6, 1972, pp. 880-886.

2. Jameson, A.: Transonic Potential Flow Calculations Using Conservative Form. Proceedings AIAA 2nd Computational Dynamics Conf., 1975, pp. 148-161.

3. Magnus, R. and Yoshihara, H.: Calculations of Transonic Flow Over an Oscillating Airfoil. AIAA Jour., Vol. 13, No. 12, 1975, pp. 1622-1628.

4. Nixon, D. and Klopfer, G. H.: Some Remarks on Transonic Potential Flow Theory. J. Appl. Mech., Vol. 50, No. 2, 1983, pp. 270-274.

5. Nixon, D.: Transonic Small Disturbance Theory with Strong Shock Waves. AIAA Jour., Vol. 18, No. 6, 1980, pp. 717-718.

6. Kerlick, G. D., Nixon, D., and Ballhaus, W. R.: Unsteady Transonic Small Disturbance Theory with Strong Shock Waves. AIAA Paper 82-0159, 1982.

7. Klopfer, G. H. and Nixon, D.: Nonisentropic Potential Formulation for Potential Flows. AIAA Paper No. 83-0375, 1983.

8. Ballhaus, W. F. and Goorjian, P. F.: Implicit Finite Difference Computations of Unsteady Transonic Flows About Airfoils Including the Effects of Irregular Shock Motions. AIAA Jour., Vol. 15, Dec. 1977, pp. 1728-1735.

9. Kwak, D.: Non-Reflecting Far Field Boundary Conditions for Unsteady Transonic Flow Computation. AIAA Jour., Vol. 19, No. 11, 1981.

10. Whitlow, W.: XTRAN2L: A Program for Solving the General Frequency Unsteady Transonic Small Disturbance Equation. NASA TM 85723, 1983.

11. AGARD Two Dimensional Aeroelastic Configurations. AGARD Advisory Report No. 156, August 1979.

In Figure (2), the steady pressure distribution and the unsteady pressure jump, $(C_p^+ - C_p^-) - (C_p^+ - C_p^-)_{steady}$ is shown for a NACA 0012 airfoil at $M_\infty = 0.8$, $\alpha_o = 0.7°$ with $\alpha_1 = 0.25°$ and $\nu = 0.6$. It may be seen that the steady state shock has moved location considerably. There is a considerable change in the unsteady pressure jump.

Figure (3) shows the steady and unsteady results for a NACA 64 A006 at $M_\infty = 0.875$ at $\alpha_o = 0.0$ with a flap deflection of 1.0° and $\nu = 0.470$; the flap hinge is at 25% of chord. This is case 10 from Ref. 11. It can be seen that while there is a relatively small change in the steady pressure distribution, there is a considerable effect in the unsteady result, mainly due to the change in location of the shock.

In Figure (4), the results are shown for the flow around a NACA 64A010 airfoil at $M_\infty = 0.796$, $\alpha_o = 0.0$ with a pitching amplitude of 1.01° and $\nu = 0.404$. The results are similar to those of the previous example. This is case 6 of Reference 11.

Finally, in Figures (5) and (6), the results for an NLR 7301 airfoil at $M_\infty = 0.721$ and $\alpha_o = -0.19°$ are shown. These are cases 8 and 13 from Reference 11. There is a double shock in this example, the first of which moves forward due to the present modifications of the method for steady flow, although the unsteady results do not differ significantly. In Figure (5), the airfoil is oscillating in pitch at $\nu = 0.362$ with amplitude 0.5°. The unsteady result differs considerably from the original result. In Figure (6), there is a flap hinged at 75% of chord oscillating at $\nu = 0.362$ with amplitude 1.0°. It should be noted that this result is for the third cycle; in the modified method the fourth cycle diverged--the reasons are not known.

4.2 Unsteady Flow

The code uses the theory outlined elsewhere except that the values of α and β are computed only on the upper and lower surfaces of the airfoil and these are used throughout the appropriate half plane. This device is for coding simplicity and assumes that the unsteady effects on the shock wave can be characterized by the behavior at the shock foot. It is also possible that instabilities in the algorithm could arise if α,β were varied along the shock. An instability did arise in the steady flow part due to varying b,c in an injudicious manner.

5. DISCUSSION OF RESULTS

One of the main purposes of the present work is to test the ideas of the present theory over a range of cases. These cases include some from Reference (10) and compare the present method with the unmodified method.

The first case is the steady flow around a NACA 0012 section at $M_\infty = 0.8$, $\alpha = 1.25°$, a case for which Euler equation solutions are available. The comparison is shown in Figure (1). It can be seen that the present result improves the agreement with the Euler solution by weakening the upper surface shock strength and moving its location forward slightly ahead of the Euler solution. A similar overcorrection is seen on the lower surface. This may be due to the strength being below the "cut off" strength, in this case $|\phi_x^+ - \phi_x^-| = 5$, and hence the present correction is not applied to the lower surface flow. It should also be noted that this solution is not fully converged, the residual being about 9×10^{-3}; however, the solution is not obviously diverging. It should also be noted that the pressure overshoot shown in the earlier work, Ref. 6, has been similarly overcorrected.

4. COMPUTATIONAL PROCEDURE

The theory developed in the preceding section was implemented in the computer code XTRAN2L (Ref. 10), as follows:

4.1 Steady Flow

When a shock appears the strength of the small disturbance shock is computed. If $|\phi_x^+ - \phi_x^-|$ is less than a specified value then no alteration is required; at present the specified value is 0.1. If the shock is sufficiently large, then the constant c is chosen to give a shock with the Rankine-Hugoniot shock strength. This is accomplished using the formulae of Equation (16). Incidently, in some of the examples the exact nonlinear formula for M_e^2 gives an imaginary value; the code was modified to use the linear equivalent formula

$$M_e^2 = M_\infty^2 + k\delta^{2/3}\phi_x$$

where k is the transonic parameter. If c is found to exceed $|b|/\delta$, then c is kept at its previous value and b is modified to achieve the correct shock strength. This reduces the likelihood of multiple parabolic points.

In order to retain a stable algorithm the coefficients b,c are updated only every 50 iterations. Furthermore, the values on the upper and lower surfaces are used throughout the respective half plane until the residual is five times the criteria for convergence or that the number of iterations exceeds 90% of the total maximum specified iterations. The correct field values are then used to increase accuracy and to allow the intermediate field solution to reduce to its classic form so that the boundary condition treatment is not compromised.

For each sweep over the airfoil the coefficients are updated only if the shock strength exceeds by 10% the strength of a previous shock calculated on the same sweep. This allows for multiple shock waves and updates the coefficients only for the first shock or the subsequent shocks if they are stronger by 10% than the first.

$$f(u) = a + bu + cu^2$$

then

$$\frac{\partial f}{\partial u} < 0 \text{ for a range of } u$$

or

$$b + 2cu < 0$$

Let u_{max} be the maximum value of u in the range, then

$$c \leq \frac{-b}{2u_{max}} \qquad c \text{ positive} \tag{30}$$

if $u_{max} = 4$, say, then

$$\frac{|c|}{|b|} \leq 1/8 \tag{31}$$

In practice a,b are approximately the same order of magnitude and hence the inequality of Equation (29) is the more restrictive. Thus,

$$c << b^2/a$$

or

$$c_{max} = \frac{1}{8} \cdot \frac{b^2}{a} \tag{32}$$

which is used in the analysis; the value "1/8" is arbitrary.

3. CONSTRAINTS ON THE COEFFICIENTS

There is a danger of the quadratic in Equation (1) term having multiple roots that are physically not unreasonable but which could destroy the algorithm stability.

The parabolic points of Equation (1) are

$$u = \frac{-b \pm [b^2 - 4ac]^{1/2}}{2c} \tag{26}$$

If $\left|\frac{c}{b}\right| << 1$ and $a \sim \underline{0}(1)$ then a Taylor's expansion gives

$$u \approx -\frac{a}{b} \quad \text{or} \quad -\frac{b}{c} + \frac{a}{b} \tag{27}$$

The proper solution is the first root since it has the correct behavior as $c \to 0$.

In order to avoid the second root it must be much larger or smaller than the first so that it is not likely to appear in a physically reasonable situation. In general, $a > 0$, $b < 0$ and $|a|$ and $|b|$ are of similar magnitude and thus

$$\left.\begin{aligned} &\text{if } -\frac{b}{c} > 0 \text{ then } -\frac{b}{c} >> -\frac{a}{b} \\ &\text{and} \\ &\text{if } -\frac{b}{c} < 0 \text{ then } -\frac{b}{c} << 0 \end{aligned}\right\} \tag{28}$$

Hence for the second root to be avoided, the following constraints must be met.

$$\left.\begin{aligned} &|c| << |b| && c \text{ negative} \\ &c << \frac{b^2}{a} && c \text{ positive} \end{aligned}\right\} \tag{29}$$

A further constraint is that the nonlinear term should be monotonic through a range of u. Thus, if

If these equations are satisfied then, to first order in shock motion, the shock will have a strength equal to the Rankine-Hugoniot value.

For steady flow a is kept equal to its traditional value, and b and c are altered to satisfy equation (16). There are some constraints on b,c and these are discussed later.

For unsteady flow, c is kept equal to its steady state value and

$$b = b_s(\phi_x^+/\phi_{x_s}^+)^{\alpha} + \beta\dot{x}_s \tag{22}$$

where the subscript s denotes a steady state value. The α and β are found by satisfying Equations (20) and (21). Thus,

$$\alpha b_s/\phi_{x_s}^+ = -\left\{b_s\left[1 - \frac{1}{2}\left(\frac{\partial\sigma_E}{\partial\phi_x^+}\right)_s\right] + c\left[2\phi_{x_s}^+ - \sigma_{Es} - \phi_{x_s}^+\left(\frac{\partial\sigma_E}{\partial\phi_x^+}\right)_s + \frac{2}{3}\sigma_{Es}\left(\frac{\partial\sigma_E}{\partial\phi_x^+}\right)_s\right]\right\}/(\phi_{x_s}^+ - \sigma_{Es}/2) \tag{23}$$

$$\beta = \left\{[b_s/2 + c\phi_{x_s}^+ - \frac{2}{3}c\sigma_{Es}]\left(\frac{\partial\sigma_E}{\partial\dot{x}_s}\right) + A\right\}/(\phi_{x_s}^+ - \sigma_{Es}/2) \tag{24}$$

where

$$\frac{\partial\sigma_E}{\partial\dot{x}_s} = -\nu\sigma_{Es}\left(\frac{2M_{e_s}^2}{M_{e_s}^2 - 1} + 1\right) \tag{25}$$

where M_{e_s} is the steady state Mach number ahead of the shock.

$$\sigma = (\phi_x^+ - \phi_x^-) = \left\{\frac{2}{(\gamma+1)M_\infty^2}(M_e^2 - 1)\left[1 + \frac{\gamma M_\infty^2}{2} C_p^+\right]\right\}/\{(1 + \nu\dot{x}_s)\delta^{2/3}\} \tag{15}$$

The problem is now reduced to replacing σ in Equation (8) with c_E.

Following the philosphy of the earlier work, the steady shock strength is fixed first. Thus,

$$a + b(\phi_{x_s}^+ - \sigma_{Es}/2) + c(\phi_{x_s}^{+2} - \phi_{x_s}^+ \sigma_{Es} + \sigma_{Es}^2/3) = 0 \tag{16}$$

This allows the constants, a, b, c to be chosen.

Next, the shock strength is expanded about its steady state value. Thus, if

$$F(\phi_x^+, \sigma, \dot{x}_s) = 0 \tag{17}$$

denotes Equation (8), then

$$F(\phi_x^+, c, \dot{x}_s) = F(\phi_{x_s}^+, \sigma_{Es}, 0) + \dot{x}_s \left(\frac{\partial F}{\partial \dot{x}_s} + \frac{\partial F}{\partial \sigma_E}\frac{\partial \sigma_E}{\partial \dot{x}_s}\right)_s$$

$$+ (\phi_x^+ - \phi_{x_s}^+)\left(\frac{\partial F}{\partial \phi_x^+} + \frac{\partial F}{\partial c_E}\frac{\partial c_E}{\partial \phi_x^+}\right) = 0 \tag{18}$$

or, since

$$F(\phi_{x_s}^+, \sigma_{Es}, 0) = 0 \tag{19}$$

$$\left(\frac{\partial F}{\partial \dot{x}_s} + \frac{\partial F}{\partial \sigma_E}\frac{\partial \sigma_E}{\partial \dot{x}_s}\right)_s = 0 \tag{20}$$

$$\left(\frac{\partial F}{\partial \phi_x^+} + \frac{\partial F}{\partial \sigma_E}\frac{\partial \sigma_E}{\partial \phi_x^+}\right)_s = 0 \tag{21}$$

where M_e is Mach number just upstream of the shock and is defined as

$$M_e=(U^+ - \dot{\bar{x}}_s)/a^+ \tag{10}$$

where $\dot{\bar{x}}_s$ is the physical shock speed, U^+ and a^+ are the velocity and speed of sound just ahead of the shock, respectively. Now

$$M_e^2 = (U^+ - \dot{\bar{x}}_s)^2/\{ a_\infty^2[1 + \frac{\gamma-1}{2} M_\infty^2(1 - U^{+2}/U_\infty^2)]\} \tag{11}$$

or

$$M_e^2 = M_{e_s}^2 (1 - \dot{\bar{x}}_s/U^+)^2 \tag{12}$$

where M_{e_s} is the steady Mach number with the steady value of U^+ replaced by its unsteady value.

In the scaled coordinate of the present problem, the physical shock speed is replaced by

$$\nu\dot{x}_s U_\infty$$

Hence,

$$M_e^2 = M_{e_s}^2 [1 - \nu\dot{x}_s/(U^+/U_\infty)]^2 \tag{13}$$

Returning now to Equation (9); if the small disturbance pressure relation,

$$C_p = -2(\phi_x^+ + 2\nu\phi_t)\delta^{2/3} \tag{14}$$

is used, then, with the help of Equation (8)

The shock jump relation is

$$\{a[\phi_x] + \frac{b}{2}[\phi_x^2] + \frac{c}{3}[\phi_x^3]\} - [\phi_y]\left(\frac{dx}{dy}\right)_s$$

$$- \{A[\phi_x] + B[\phi_t]\}\left(\frac{dx}{dt}\right)_s = 0 \tag{4}$$

where [ ] denotes a jump across the shock. Since $(dx/dt)_s = \dot{x}_s$, the shock speed, is continuous through the shock, then

$$[\phi_t] = [\phi_x]\dot{x}_s \tag{5}$$

and hence for a normal shock Equation (4) becomes

$$\{a + \frac{b}{2}(\phi_x^+ + \phi_x^-) + \frac{c}{3}(\phi_x^{+2} + \phi_x^+\phi_x^- + \phi_x^{-2})\} - \dot{x}_s\{A + B\dot{x}_s\} = 0 \tag{6}$$

If a shock strength, σ, is defined by

$$\sigma = \phi_x^+ - \phi_x^- \tag{7}$$

Then Equation (6) becomes

$$\{a + b(\phi_x^+ - \sigma/2) + c(\phi_x^{+2} - \phi_x^+\sigma + \sigma^2/3)\}$$

$$- \dot{x}_s\{A + B\dot{x}_s\} = 0 \tag{8}$$

Consider now the one-dimensional Euler shock strength. The pressure jump is given by

$$\frac{p^-}{p^+} - 1 = \frac{2\gamma}{\gamma+1}(M_e^2 - 1) \tag{9}$$

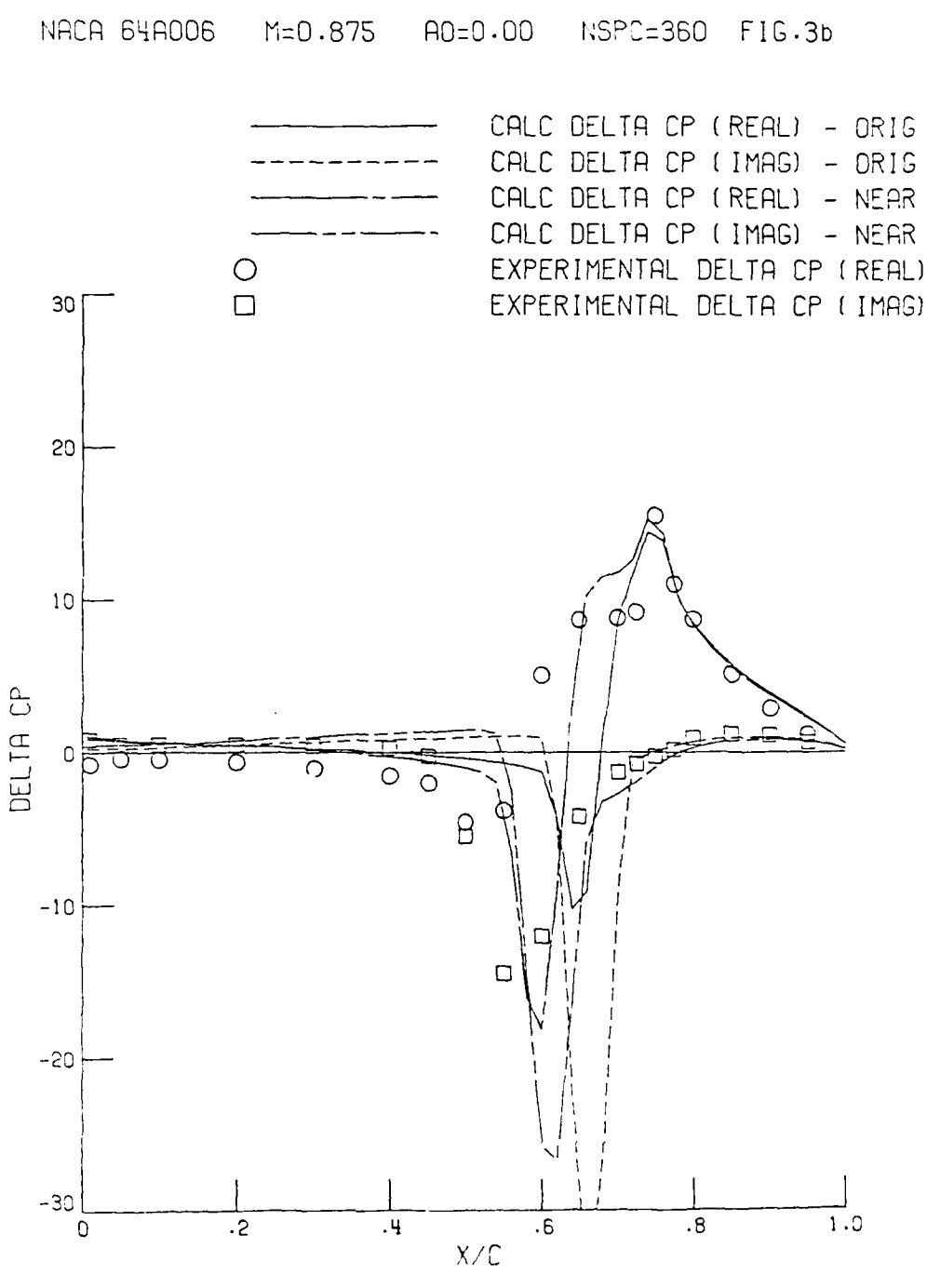

(b) Unsteady flow, $\delta_1 = 1.0°$

Figure 3.- Concluded.

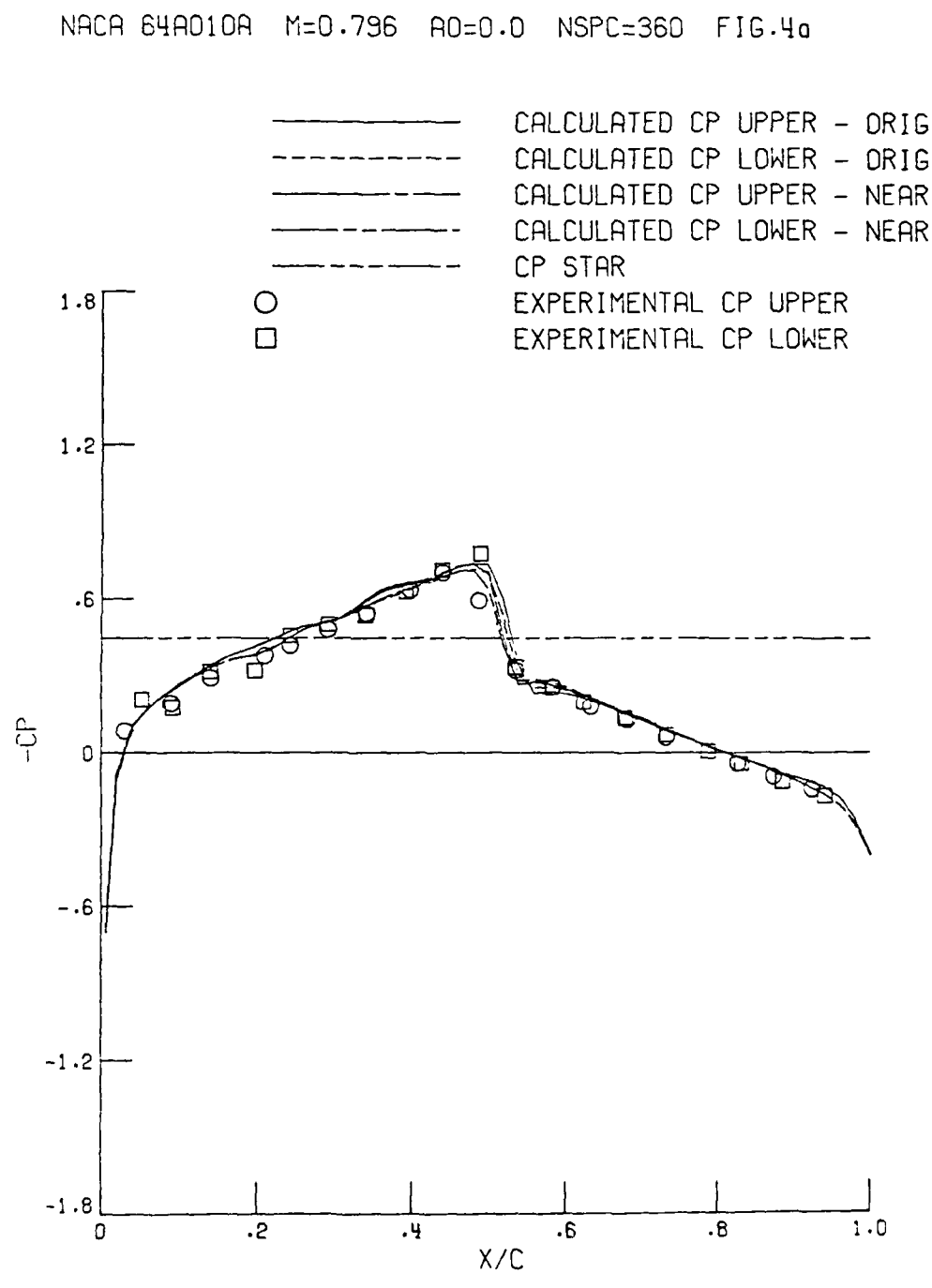

(a) Steady flow, $\alpha_0 = 0.0$

Figure 4.- Pressure distributions around a NACA 64A010 airfoil, $M_\infty = 0.796$.

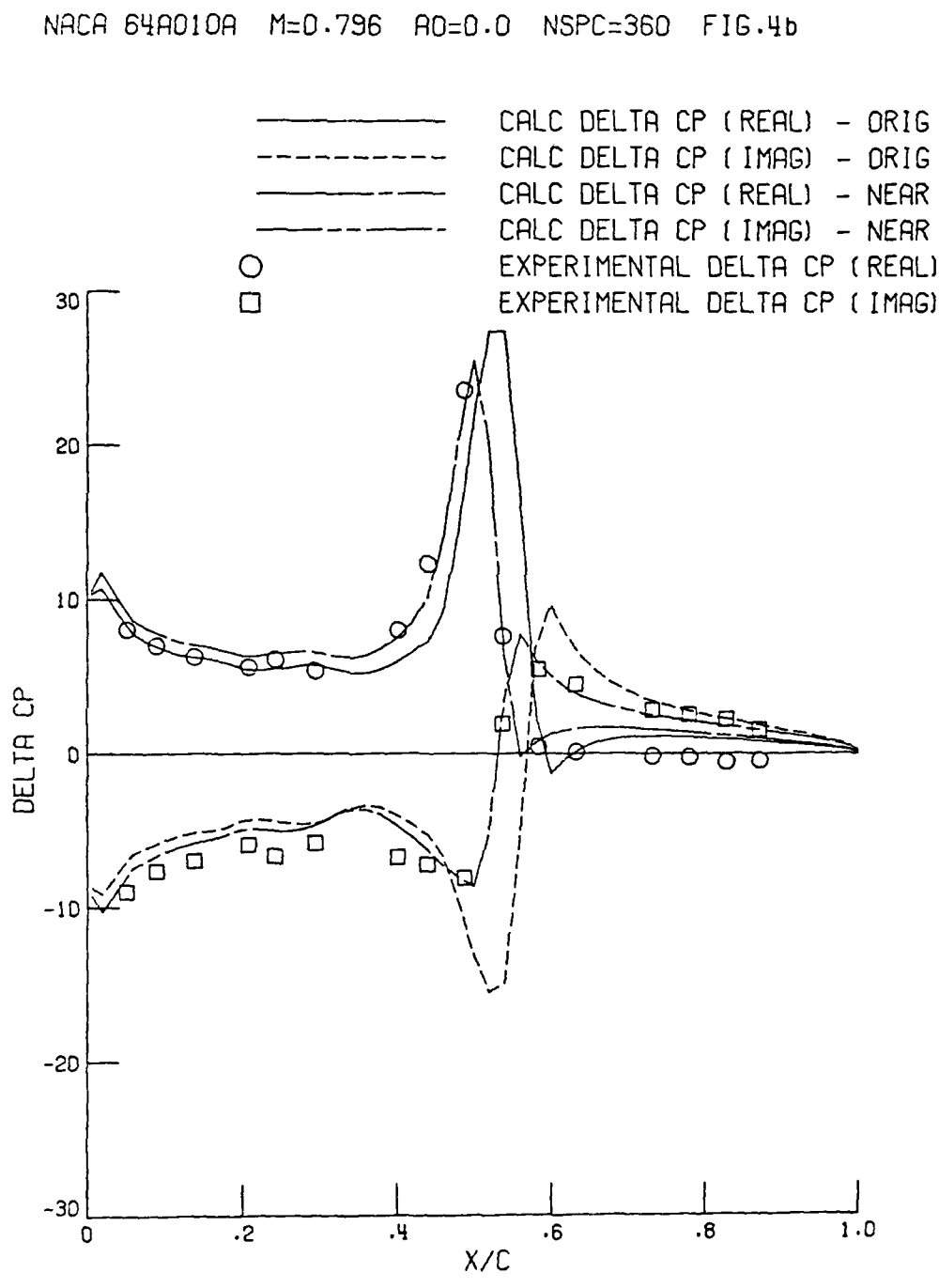

(b) Unsteady flow, $\alpha_1 = 1.01°$

Figure 4.- Concluded.

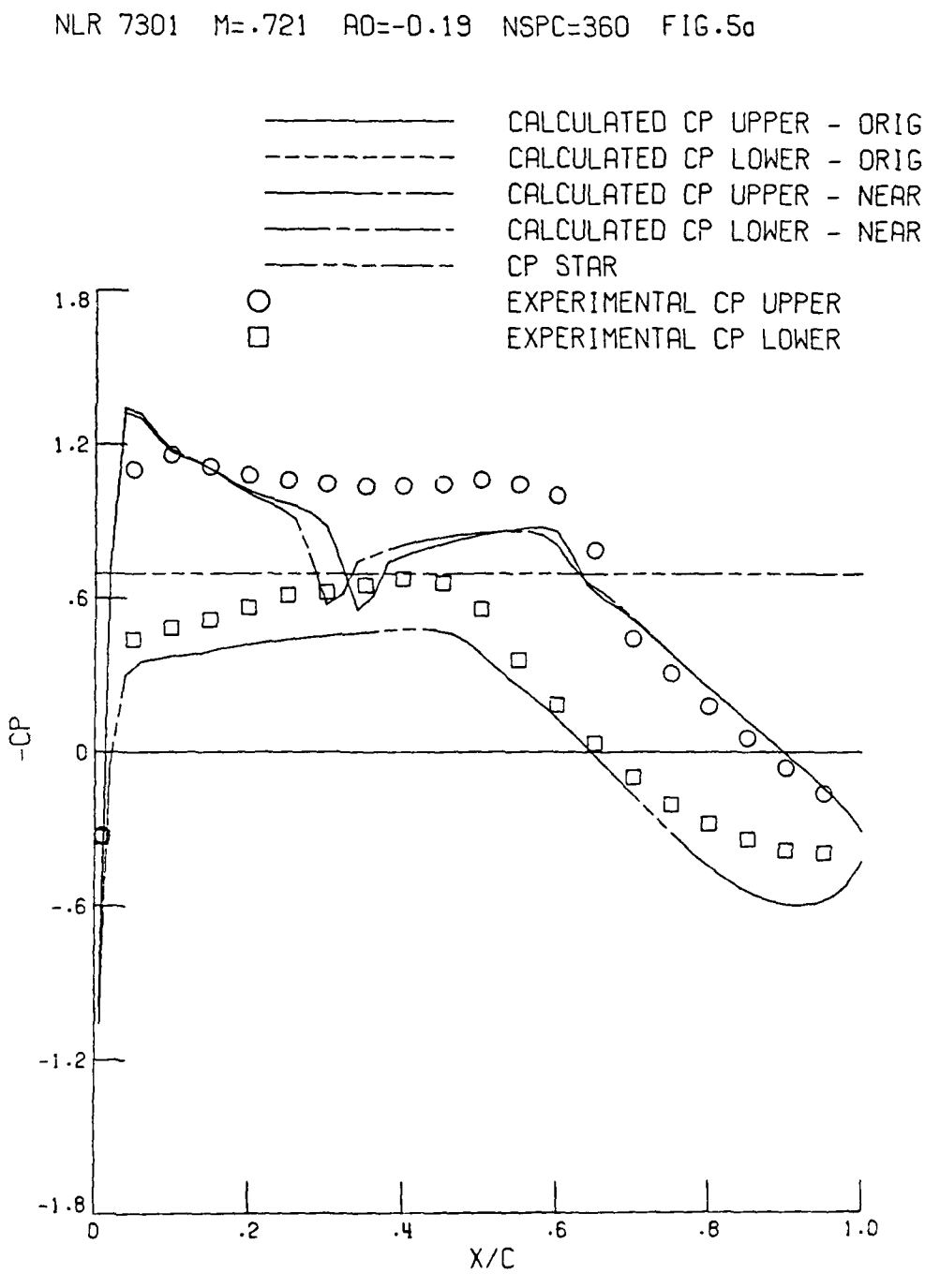

(a) Steady flow, $\alpha_0 = -0.19°$

Figure 5.- Pressure distributions around a NLR 7301 airfoil, $M_\infty = 0.721$.

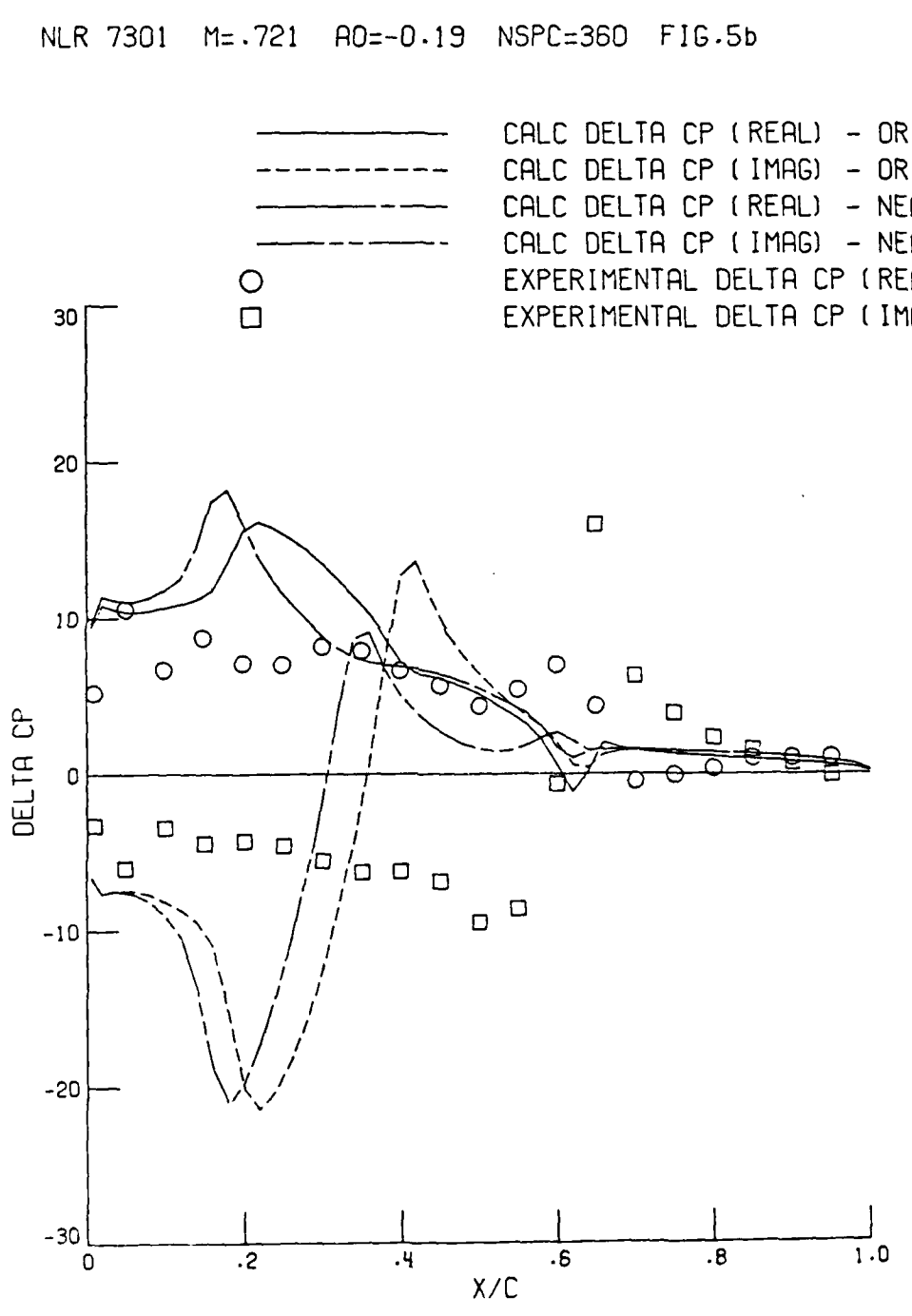

(b) Unsteady flow, $\alpha_1 = 0.5°$

Figure 5.- Concluded.

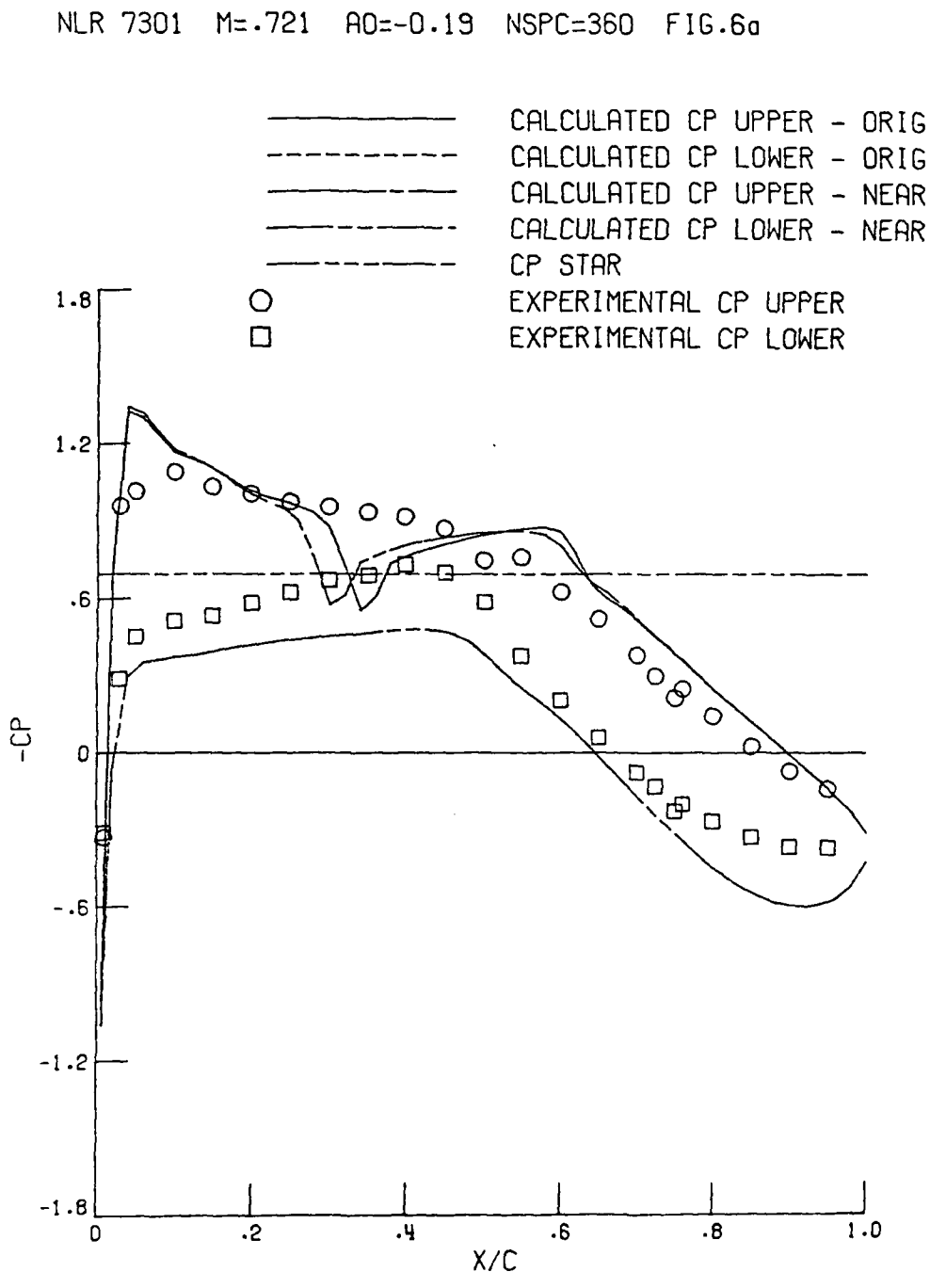

(a) Steady flow, $\alpha_0 = -0.19°$

Figure 6.- Pressure distributions around a NLR 7301 airfoil, $M_\infty = 0.721$.

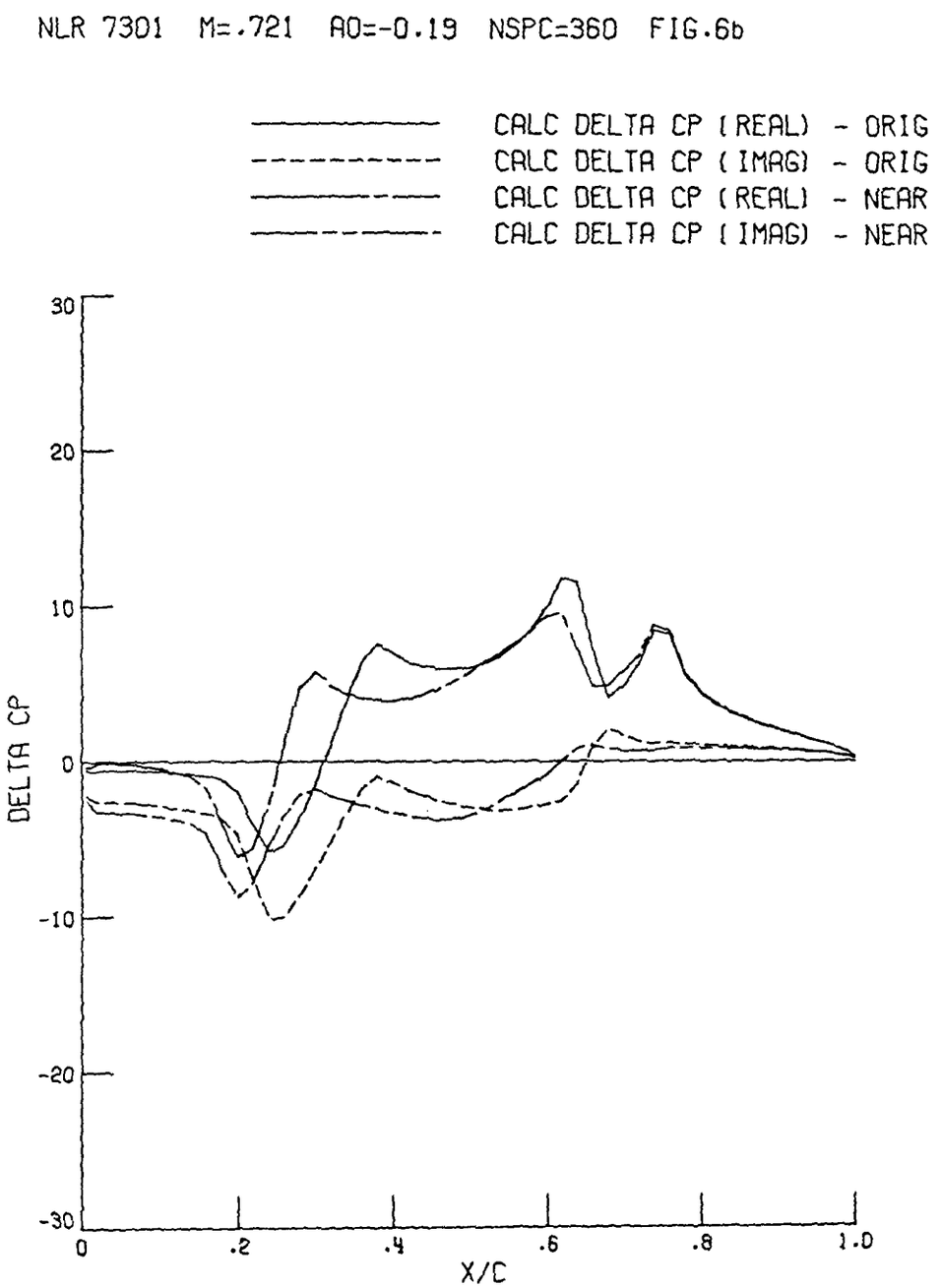

(b) Unsteady flow, $\alpha_1 = 1.0°$

Figure 6.- Concluded.

APPENDIX

NOTES ON THE EXTENSION OF THE KLOPFER-NIXON METHOD TO UNSTEADY FLOW

In Reference 7 a method is developed to modify the steady full potential equation to treat strong shock waves. The results of this method agreed better with solutions of the Euler equations than the steady version of Reference (6) and it is therefore instructive to see whether some of these ideas can be extended to time dependent flows.

Consider the two dimensional Euler equations:

$$\frac{\partial \rho}{\partial t} + \frac{\partial \rho u_i}{\partial x_i} = 0 \tag{1}$$

$$\frac{\partial \rho u_i}{\partial t} + \frac{\partial \rho u_i u_j}{\partial x_j} = - \frac{\partial p}{\partial x_i} \tag{2}$$

$$\frac{\partial H}{\partial t} + u_i \frac{\partial H}{\partial x_i} = 0 \tag{3}$$

where

$$H = h + \frac{1}{2} u_i u_i \quad ; \quad h = \frac{\gamma}{\gamma - 1} p/\rho \tag{4}$$

For steady isentropic flow the energy equation can be integrated along a streamline to give

$$h + \frac{1}{2} u_i u_i = \text{constant} = h_o \tag{5}$$

and the isentropic relation

$$p/\rho^\gamma = \text{constant} = k\, p_\infty/\rho_\infty^\gamma \tag{6}$$

can be used to give

$$\rho = \rho_\infty \left[1 + \frac{\gamma - 1}{2} M_\infty^2 \left(1 - \frac{u_i u_i}{q_\infty^2} \right) \right]^{\frac{1}{\gamma - 1}} / k^{\frac{1}{\gamma - 1}} \tag{7}$$

This relation is then used in conjunction with the conservation of mass equation and the irrotationality equation

$$u_i = \frac{\partial \phi}{\partial x_i} \tag{8}$$

To give an equation for ϕ. In the usual case k = 1 but for the strong shock case, k is allowed to jump at the shock wave.

For unsteady flow the energy equation cannot be integrated and the necessary density/velocity relation is obtained from the momentum equation.

Consider the x momentum equation in two dimensions

$$\frac{\partial u}{\partial t} + \frac{u\partial u}{\partial x} + \frac{v\partial u}{\partial y} = -\frac{1}{\rho}\frac{\partial p}{\partial x} \tag{9}$$

Using irrotationality and the isentropic relation gives

$$\frac{\partial}{\partial x}\left\{\frac{\partial \phi}{\partial t} + \frac{1}{2}(u^2 + v^2) + \frac{p_\infty}{\rho_\infty}\frac{\partial}{\partial x}\left[k(\rho/\rho_\infty)^\gamma\right]\right\} = 0 \tag{10}$$

If k is constant, then Equation (10) reduces to the form

$$\frac{\partial}{\partial x}\left\{\frac{\partial \phi}{\partial t} + \frac{1}{2}(u^2 + v^2) + \frac{\gamma p_\infty}{(\gamma-1)\rho_\infty} k \left(\frac{\rho}{\rho_\infty}\right)^{\gamma-1}\right\} = 0 \tag{11}$$

which can be integrated to give the unsteady Bernoulli equation. If k is allowed to jump through the shock then the equation is

$$\frac{\partial}{\partial x}\left\{\frac{\partial \phi}{\partial t} + \frac{1}{2}(u^2 + v^2) + \frac{\gamma}{\gamma-1}\frac{p_\infty}{\rho_\infty} k \left(\frac{\rho}{\rho_\infty}\right)^{\gamma-1}\right\} + \frac{\gamma p_\infty}{\rho_\infty}\left(\frac{\rho}{\rho_\infty}\right)^{\gamma-1}\frac{\partial k}{\partial x} = 0 \tag{12}$$

which does not give a simple density/velocity relation. Thus, the application of the theory of Ref. 7 to unsteady flow is more difficult than first envisaged.

APPENDIX 2

OBSERVATIONS ON THE OCCURENCE OF MULTIPLE SOLUTIONS IN TRANSONIC POTENTIAL THEORY

by

David Nixon

NIELSEN ENGINEERING & RESEARCH, INC.
Mountain View, CA 94043

1. INTRODUCTION

In recent years multiple solutions to the numerical approximation to the full potential equations have appeared in the literature (Refs. 1 and 2). Initially the phenomena appeared in computations of the flow over a symmetric airfoil at zero angles of attack whre two lifting solutions were present in addition to the expected nonlifting solution. In Reference 2 some results, for a nonsymmetric airfoil, a RAE 2822 section, are also presented. Steinhoff and Jameson (Ref. 1) suggested that the change from one of the solutions to another is discontinuous and noted a hysteresis effect indicating that the lift coefficient (C_L) depended on whether the angle of attack (α) was increasing or decreasing. More recent work is by Salas (Ref. 2) who has extended the computations of the flows considered by Steinhoff and Jameson (Refs. 1) to show that it is possible to construct a smooth C_L - α curve connecting the three solutions for a symmetric airfoil.

The investigations noted above are meticulously performed and are essentially numerical experiments. There is a limited amount of understanding that can be gained from such experiments and consequently a more analytic technique may yield additional information. Furthermore, although the numerical results are invaluable they do not exclude the possibility that the multiple solutions are due to the numerical approximation to the differential equation. The present investigation is based on the integral equation formulation (Ref. 3) which allows some degree of insight into the problem.

The objective of this paper is to suggest a possible reason for the multiple solutions based on the existence of an eigensolution in the transonic small disturbance (TSD) equation. It is shown that a ficticious lift can be added to a

"real" solution to give a multiple of solutions. It is also indicated that the methods used to stabilize a numerical solution are likely to indicate the appearance of the eigensolution.

2. INTEGRAL EQUATION ANALYSIS

The transonic integral equation method of Reference 3 is only applicable to the transonic small disturbance (TSD) equation rather than the full potential equation (FPE) that is used in the earlier work. Consequently the first step is to reproduce multiple solutions using the TSD equation. Once these solutions are obtained they can be analyzed using the ideas of the transonic integral equation theory.

2.1 Multiple Solutions for Small Disturbance Theory

Since it is easiest at present to use the integral equation theory to analyze small disturbance theory it is necessary to reproduce the multiple solutions using the TSD equation. This is achieved by using the computer code TSFOIL (Ref. 4) which solves the TSD equation using the conservative Murman-Cole algorithm and grid sequencing. The multiple solutions are found for a symmetric airfoil at zero angle of attack by imposing a 1° angle of attack on the coarse grid solution and then putting the angle of attack equal to zero in the medium and fine grid operations. It is found that such a device leads to multiple solutions over a small range of Mach numbers. Such solutions have been found for a 11.8% Joukowski airfoil and a NACA 0012 airfoil. As a test for convergence, the solution for the Joukowski airfoil at $M_\infty = 0.85$ was converged to a residual of 10^{-9}. Krupp scaling was used in these results; the default Krupp grid is used, which has grid dimensions of 77 x 56. An example of a multiple solution is given in Figure 1.

2.2 Transonic Integral Equation Theory

Since the analysis of the multiple solutions is based on the integral equation theory it is helpful to outline the formulation.

For Krupp scaling the TSD equation can be written as

$$(1 - \phi_x)\phi_{xx} + \phi_{yy} = 0 \tag{1}$$

where if $\bar{\phi}$ is the perturbation velocity potential in a Cartesian coordinate system $(\bar{x},\bar{y})$ then

$$\begin{aligned} \phi &= \frac{k}{\beta^2}\bar{\phi} \\ x &= \bar{x} \\ y &= \beta\bar{y} \end{aligned} \tag{2}$$

where

$$\begin{aligned} k &= (\gamma + 1)M_\infty^{1.75} \\ \bar{v} &= (\beta^3/k)v \end{aligned} \tag{3}$$

If $u = \phi_x$, $v = \phi_y$ then the physical perturbation velocity components $(\bar{u},\bar{v})$ are given by

$$\begin{aligned} \bar{u} &= (\beta^2/k)u \\ \bar{v} &= (\beta^3/k)v \end{aligned} \tag{4}$$

In the formulation of Equation (1) the sonic line is given by

$$u = \phi_x = 1 \tag{5}$$

The boundary conditions for Equation (1) are that $\phi_x, \phi_y \to 0$ on the far field, that the tangency condition

$$\phi_y(x,\pm 0) = y_s'(x,\pm 0) - \bar{A} \tag{6}$$

It is of interest to note that if a stabilizing term of the type used in TSFOIL, namely $\varepsilon\phi_{xt}$ is added to Equation (1), where t is an artificial iteration time and ε is a parameter, then an analysis similar to that given in this section shows that this term will assist the formation of a nonunique solution. This is possibly the reason why the real solution cannot sometimes be computed. The same effect is also present if the dissipation due to the truncation error in the upwind difference scheme is indicated in the analysis. In other words, a stable conservative algorithm is likely to initiate the appearance of the eigensolution g in the solution.

3. SUMMARY

The TSD equation can admit eigensolutions that satisfy all of the boundary conditions generally found in such problems; there are an infinite number of these eigensolutions. For a nonunique solution to exist certain consistency requirements must be met. These eigensolutions provide lift and act like an additional asymmetric source term in the flow field. If real lift is present the fictitious component provided by the nonuniqueness appears as a simple additive term to the real lifting component; there is no way to distinguish or uncouple the two components in a given numerical solution.

If, in a supercritical flow, an eigensolution does appear, the location of the shock waves changes from their real location. The nonuniqueness may be removed in some steady cases by using a nonconservative/conservative algorithm which may inhibit the appearance of such solutions. However, there is no guarantee that this will work in all cases. This partial cure only works for steady flows; it is possible that for unsteady flows that a "strong shock" theory of the type advocated in Reference 8 could remove any nonuniqueness. The (necessary)

lower surface shock moves forward. It follows that the source term introduced by the shock on the lower surface now acts at a further forward location while the countering source on the upper surface moves aft. Consequently, there is a considerable region between the shocks for which

$$\Delta[\sigma_i H(x-x_{s_i})] < 0$$

This counters the positive g and reduces the tendency of the nonunique solution to appear. However, it is necessary to point out that the nonconservative source error must be large enough to counter the g terms. The nonconservative algorithm only inhibits a nonunique solution from appearing; it will not necessarily remove an existing error. A similar analysis can be performed if the fictitious lift is negative. This hypothesis was tested by using the computer code TSFOIL (Ref. 4) which has both conservative and nonconservative algorithms. A composite algorithm, given by

$$\text{Algorithm} = \lambda\ (\text{conservative}) + (1 - \lambda)\ (\text{nonconservative}) \qquad (65)$$

was used. The parameter, λ, was taken to be given by

$$\lambda = -\varepsilon\left|[C_L(t+\Delta t) - C_L(t)]\right| + 1 \qquad (66)$$

where t is the artificial iteration time and Δt is the iteration step. At convergence $\lambda = 1$ and the solution is conservative. It was found that for the nonunique solutions to be avoided in a computation of the example in Figure 1 $\varepsilon[C_L(t+t\Delta t) = C_L(t)]$ had to be of order unity during most of iteration. Smaller values did not inhibit nonuniqueness. Hence it is suggested that the "classic" degree of nonconservative algorithm is necessary to stop the appearance of nonunique solutions.

It is of interest to note that the foregoing analysis is based on the boundary conditions of Equations (6) which are in similarity form. Hence a nonunique solution can appear for a range of thickness and camber parameters provided the Mach number is changed so that the similarity boundary conditions are unchanged. This is consistent with the numerical evidence of Salas et al. (Ref. 2).

2.7 Non-Conservative Algorithms

A non-conservative algorithm, such as that of Murman and Cole (Ref. 7) adds source terms at the shock waves. Hence the algorithm is solving conservatively a differential equation of

$$(1-\phi_x)\ \phi_{xx} + \phi_{yy} = [\sigma_i H(x - x_{s_i})]_x \qquad (60)$$

where $\sigma_i(y)$ is a source term at the shock location x_{s_i} and $H(\ )$ is the step function. The strength of the source term is not known explicitly in non-conservative algorithms.

If the asymmetric part of Equation (60) is taken then

$$\Delta\phi_{xx} + \Delta\phi_{yy} = (\Delta u\bar{u})_x + \Delta[\sigma_i H(x-x_{s_i})]_x \qquad (61)$$

If Equation (61) is added to Equation (44) the following result is obtained.

$$(\Delta\phi+G)_{xx} + (\Delta\phi+G)_{yy} = (\Delta u\bar{u})_x + \{g + \Delta[\sigma_i H(x-x_{s_i}]\}_x \qquad (62)$$

If a ficticious positive component of lift starts to appear in a solution, g will change from zero to a predominantly positive quantity, since g is equivalent to $(\Delta u\bar{u})$. This introduction of positive lift will change the location of the shock waves such that an upper surface shock moves aft while a

If there is a real lift due to the boundary condition of Equation (6) then Equation (24) gets replaced by

$$\int_{S_1}\int K_{\xi y}[f+f^* - I_{c_L}]d\xi d\eta \tag{57}$$

where I_{c_L} is given by Equation (28) and f* is a function that satisfies

$$\int_{S_1}\int [f^* - I_{c_L}]d\xi d\eta = 0 \tag{58}$$

and

$$f^* \neq I_{c_L}$$

The analysis described above is unchanged if f is replaced by $f + f^*$ since f always occurs as part of the term $f + f^*$; in this case $f + f^*$ must satisfy Equation (57) rather than Equation (24). Also, since f^* alone will satisfy Equations (56) and (57) there must be at least two consistent solutions for $f + f^*$ for multiple solutions to exist.

Equation (56) can be written as

$$\left(\frac{g}{g+I_f} + I_f + g\right) - \frac{1}{2}\left(\frac{g}{g+I_f} + I_f + g\right)^2 = u_{LS} + u_{LA} - \frac{1}{4\pi}\int_{S_1}\int K_{x_s}\left[\frac{g}{I_f+g+g+I_f}\right]^2 d\xi d\eta \tag{59}$$

where

$$U_{LA} = \int_o^1 \frac{-f_o/(1-\bar{u}_o)\ y}{(x-\xi)^2 + y^2}\, d\xi$$

Since the addition of the u_{LA} term has the same effect as introducing camber into the airfoil a nonunique solution generally will have a different shock location than a real solution.

$$\bar{u} = \frac{g}{g + I_f} \tag{53}$$

it also follows from Equation (53) that

$$\Delta u = g/\bar{u} = g + I_f \tag{54}$$

From Equation (34)

$$\Delta u_o = \frac{fo}{\bar{u}_o - 1}$$

and if the limit as $y \to 0$ is taken of Equation (31) and if Equations (53) and (54) are used then

$$\bar{u}_o - \frac{\bar{u}_o^2}{2} u_{LS_o} + \frac{1}{2}\left(\frac{fo}{u_o - 1}\right)^2 - \frac{1}{4\pi} \lim_{y \to 0} \int_{S_1} \int K_{\xi x} \left[\frac{g^2}{(g+I_f)^2} + (g+I_f)^2\right] d\xi d\eta \tag{55}$$

where u_{LS_o} is the value of U_{LS} at $y = 0$.

Since f is assumed known and U_{LS_o} is known, Equation (55) is an equation for $\bar{u}_o$. Hence g can be found.

Using Equations (58) and (59) to eliminate $\bar{u}$ and Δu in Equation (33) it follows that a nonunique solution only exists if there is a solution f, to the equation

$$\frac{g}{g+I_f} - \frac{1}{2}\left(\frac{g}{g+I_f}\right)^2 = u_{LS} + \frac{1}{2}(g+I_f)^2 - \frac{1}{4\pi} \int_{S_1} \int K_{x\xi} \left[\frac{g^2}{(g+I_f)^2} + (g+I_f)^2\right] d\xi d\eta \tag{56}$$

This solution must also satisfy Equation (24). For a real nonlifting case a nonunique solution will appear if a nonzero value of f satisfies both Equations (24) and (56).

(49) are similar in form to Equations (1) and (6) if ϕ is identified with $\bar{\phi} + G$. . The numerical algorithm will solve Equation (48) in an identical manner to the real solution.

If there is real lift, that is a value that is calculated with no eigensolutions, then the lifting solution of Equation (38) can be added to Equation (48) to give

$$(\bar{\phi} + \Delta\overset{*}{\phi}+G)_{xx} + (\bar{\phi} - \Delta\overset{*}{\phi}+G)_{yy} = \frac{1}{2}\left[(\bar{u} + \Delta u + \frac{\overset{*}{g}}{\bar{u}})^2\right]_x \qquad (50)$$

where "*" denotes a real lifting component. In this case Δu on the right hand side of Equation (41) is identified with $[\Delta u^* + g/\bar{u}]$.

The boundary condition is

$$\bar{\phi}_y(x,\pm 0) + \Delta\phi^*_y(x,\pm 0) + G_y(x,\pm 0) = Y'_s(x,\pm 0) - \bar{A} \qquad (51)$$

Again a ficticious lifting component G(x,y) is added to the equation without a change in the boundary conditions. If G is present the numerical algorithm will solve Equation (50) in an identical manner as the real solution. It is not possible to decouple the real and ficticious components.

In the preceeding analysis $\bar{u}$ has been assumed known. For a solution to exist it also must be a solution of Equation (31).

Equation (37) can be written as

$$\left(\frac{1-\bar{u}}{\bar{u}}\right) g = -\frac{1}{4\pi}\int_{S_1}\int K_{\xi x}\, f\, d\xi d\eta = I_f \qquad (52)$$

where g is given by Equation (46). It follows from Equation (52) that

Now Equation (37) can be modified to give the integral equation

$$\frac{q}{\bar{u}} = g + \frac{1}{2\pi}\int_{\infty}^{\infty} \frac{fo/(1-u_o)y}{(x-\xi)^2+y^2}d\xi - \frac{1}{4\pi}\int_{S_1}\int K_{\xi x} g\, d\xi\, d\eta \qquad (43)$$

which can be written in differential form as

$$G_{xx} + G_{yy} = g_x \qquad (44)$$

where

$$G(x,y) = \int^{x} \frac{1}{\bar{u}(\xi,y)}\, g\,(\xi,y)\, d\xi \qquad (45)$$

and

$$g(\xi,y) = f(\xi,y) - \frac{f(\xi,0)}{1-\bar{u}(\xi,o)} \qquad (46)$$

with the boundary condition

$$G_y(x,\pm 0) = 0 \qquad (47)$$

In the far field G behaves like a point vortex.

If G(x,y) is identified with a lifting term $\Delta\phi$ then Equations (41) and (44) can be added to give

$$(\bar{\phi} + G)_{xx} + (\bar{\phi} + G)_{yy} = \frac{1}{2}\left[\bar{u} + \frac{g}{\bar{u}}\right]^2_x \qquad (48)$$

$$\bar{\phi}_y(x,\pm 0) + G_y(x,\pm 0) = \frac{1}{2}\left[Y'_s(x,+0) - Y'_s(x,-0)\right] \qquad (49)$$

where Δu on the right hand side of Equation (41) has been identified as $g\sqrt{u}$. Thus a ficticious value, G, can be added to a purely symmetric problem, denoted by $\bar{\phi}$, to give lift; the boundary conditions are not affected. This is the mechanism of the appearance of the nonunique solutions. Equations (48) and

(32). Hence for a nonunique solution to exist Δu, as defined by Equation (35) must be compatible with Equation (32).

Substitution of Equation (33) into Equation (32) gives

$$\Delta u - \Delta u_o = f - \frac{1}{4\pi} \int_{S_1} \int K_{\xi x} f \, d\xi d\eta \tag{36}$$

or, using Equations (34), (35)

$$\frac{1}{\bar{u}} \left[f - f_o \frac{(1-\bar{u})}{(1-\bar{u}_o)} \right] = f - \frac{1}{4\pi} \int_{S_1} \int K_{\xi x} f \, d\xi d\eta \tag{37}$$

The basic differential equation, (1), can be decoupled into symmetric and asymmetric parts. The asymmetric part is

$$\Delta\phi_{xx} + \Delta\phi_{yy} = (\Delta u \bar{u})_x \tag{38}$$

where

$$\Delta\phi(x,y) = \frac{1}{2} \left[\phi(x,y) - \phi(x,-y) \right] \tag{39}$$

the boundary condition is

$$\Delta\phi_y(x,o) = -\bar{A} + \frac{1}{2} \left[Y_s'(x,+0) + Y_s'(x,-0) \right] \tag{40}$$

The symmetric part is

$$\bar{\phi}_{xx} + \bar{\phi}_{xx} = \frac{1}{2} \left[\bar{u}^2 + \Delta u^2 \right]_x \tag{41}$$

with

$$\bar{\phi}_y(x,o) = \frac{1}{2} \left[Y_s'(x,+0) - Y_s'(x,-0) \right] \tag{42}$$

Equation (10) can be manipulated to give the following symmetric and asymmetric parts.

$$\bar{u}(x,y) - \frac{1}{2}\left[\bar{u}^2(x,y) + \Delta u^2(x,y)\right] = u_{L_S} - \frac{1}{4\pi}\int_{S_1}\int K_{\xi x}\left[\bar{u}^2(\xi,\eta) + \Delta u^2(\xi,\eta)\right]d\xi d\eta \qquad (31)$$

$$\Delta u(x,y) - \Delta u(x,y)\bar{u}(x,y) = -\frac{1}{4\pi}\int_{S_1}\int k_{\xi x}\left[u^2(\xi,\eta) - u^2(\xi,\eta) - 2\Delta u(\xi,o)\right]d\xi d\eta \qquad (32)$$

These equations will be used in the following sections.

2.6 Analysis of Multiple Solutions

If in Equation (24), $f(\xi,\eta)$ is known then Equation (23) gives

$$\frac{1}{2}\left[u^2(\xi,\eta) = u^2(\xi,\eta) - 2\Delta u(\xi,0)\right] = \Delta u(\xi,\eta)\bar{u}(\xi,\eta) - \Delta u(\xi,0) - f(\xi,\eta) \qquad (33)$$

If $\bar{u}(\xi,\eta)$ is known then this is an equation for $\Delta u(\xi,\eta)$ in the flow field and gives

$$\Delta u_o = \frac{f_o}{\bar{u}_o - 1} \qquad (34)$$

where

$$f_o = f(\xi,0) \text{ etc.;}$$

also

$$\Delta u = \frac{f + \Delta u_o}{\bar{u}} = \frac{1}{\bar{u}}\left[f - \frac{f_o}{1-\bar{u}_o}\right] \qquad (35)$$

In the transonic solution Equation (16) only gives the value of $\Delta u(\xi,o)$ or Δu_o, the value of $\Delta u(x,y)$ being found from Equation

where for $0 < x < 1$

$$I_{c_L}(x) = \frac{1}{\pi}\left(\frac{1-x}{x}\right)^{1/2}\int_0^1 \frac{-\bar{A} + \frac{1}{2}\left[Y_s'(\xi) + Y_s'(\xi)\right]}{(x-\xi)}\left(\frac{\xi}{1-\xi}\right)^{1/2} d\xi \tag{28}$$

and

$$I_{c_L}(x) = 0;\ x < 0,\ x > 1;$$

$u(\xi,\eta)$ is a transonic solution subject to the arbitrary boundary conditions in Equation (6). Since the boundary condition is arbitrary, and therefore an infinite number of boundary conditions can be applied, it follows that an infinite number of solutions $u(\xi,\eta)$ exist.

Equation (28) is identical in form to Equation (24) with $f(\xi,\eta)$ given by.

$$f(\xi,\eta) = u^2(\xi,\eta) - u^2(\xi,-\eta) - 2\Delta u(\xi) - 2I_{c_L}(\xi) \neq 0 \tag{29}$$

Since there are an infinite number of transonic solutions it follows that there are an infinite number of eigensolutions $f(\xi,\eta)$. A justification of a nonzero $f(\xi,\eta)$ is given in the Appendix.

2.5 Symmetric and Antisymmetric Integral Equations

Let $\bar{u}(\xi,\eta)$ and $\Delta u(\xi,\eta)$ be defined by

$$\bar{u}(\xi,\eta) = \frac{1}{2}\left[\bar{u}(\xi,\eta) + \bar{u}(\xi,-\eta)\right] \tag{30a}$$

$$\Delta u(\xi,\eta) = \frac{1}{2}\left[\bar{u}(\xi,\eta) + \bar{u}(\xi,-\eta)\right] \tag{30b}$$

$$\int_S \int k_{\xi y} [u^2(\xi,\eta) = u^2(\xi,\eta) - 2\Delta u(\xi)] d\xi d\eta = 0 \qquad (23)$$

where S_1 covers half of the domain S. Equation (23) can be written in the more compact form.

$$\int_S \int_1 k_{\xi y} f(\xi,\eta) d\xi d\eta = 0 \qquad (24)$$

where

$$f(\xi,\eta) = [u^2(\xi,\eta) = u^2(\xi,-\eta) = 2\Delta u(\xi)]$$

One solution of this integral equation is

$$f(\xi,\eta) = 0 \qquad (25)$$

which is the symmetric solution for the airfoil problem. A nonsymmetric solution can be obtained if there is one or more functions $f(\xi,\eta) = / 0$ that satisfy Equation (24). If there are such solutions then a multiple solution in transonic flow can exist if the equation

$$\frac{1}{2} [u^2(\xi,\eta) = u^2(\xi,-\eta) - 2\Delta u(\xi)] = f(\xi,\eta) \qquad (26)$$

has a real solution for $u(\xi,\eta)$.

2.4 Existence and Nature of Eigensolutions

It is desirable to determine the existence and the nature of the eigensolutions, $f(\xi,\eta)$ of Equation (24). Consider Equations (16) and (18). Using the inversion procedure that leads to Equation (20), Equations (16), (18) can be written in the form

$$\int_{S_1} \int K_{\xi y} [(u^2(\xi,\eta) - u^2(\xi,-\eta) - 2\Delta u(\xi) - 2I_{c_L}(\xi)] d\xi\eta = 0 \qquad (27)$$

This integral equation is valid for shock waves normal to the freestream; if the shocks are not normal to the freestream a modified integral equation is used (Ref. 6). Since the formulation changes are negligible the above set of equations will be used in the subsequent discussions for clarity.

In the solution of the integral equations the circulation is given by Equation (16) although it should be emphasized that Equations (10) and (16) are not independent. The solution of Equation (16) is found by inverting the integral equation to give

$$\Delta u(x) - \frac{\Delta u^2(x)}{2} = u_{LA}(x,0) - \frac{1}{\pi}\left(\frac{1-x}{x}\right)^{1/2} \int_0^1 \frac{I_c(\xi)}{x-\xi} \cdot \left(\frac{\xi}{1-\xi}\right)^{1/2} d\xi \tag{20}$$

where u_{LA} is the antisymmetric solution of Equation (1) without the nonlinear terms and is given by

$$u_{LA}(x,0) = \frac{1}{\pi}\left(\frac{1-x}{x}\right)^{1/2} \int_0^1 \frac{-\bar{A} + \frac{1}{2}\left[Y_s'(\xi,+0) + Y_s'(\xi,-0)\right]}{(x-\xi)} \left(\frac{\xi}{1-\xi}\right)^{1/2} d\xi \tag{21}$$

The inversion procedure invokes the Kutta condition.

2.3 Application of the Integral Equations to Multiple Solutions

Consider for the moment the case of a symmetric airfoil at zero angle of attack in this case

$$\begin{aligned} \bar{A} &= 0 \\ Y_s(x,+0) &= -Y_s(x,-0) \end{aligned} \tag{22}$$

and the left hand side of Equation (16) is zero. A manipulation of the integrals in Equation (16) leads to the equation

where

$$\Delta u(\xi) = [u(\xi,+0) = u(\xi,-0)]/2 \tag{13}$$

The Kernel function $K(x,\xi;y,\eta)$ is given by

$$K(x,\xi;y,\eta) = \frac{1}{2} \ln [(x - \xi)^2 + (y - \eta)^2] \tag{14}$$

The integral I_T is given by

$$I_T(u) = - \frac{1}{4\pi} \int_S \int K_{\xi x}(x,\xi;y,\eta) u^2(\xi,\eta) dS \tag{15}$$

The domain S is shown in Figure 2.

If $y = \pm 0$, Equation (10) gives (see Ref. 5) only the symmetric part of the solution and the antisymmetric part is given by

$$-\bar{A} + \frac{1}{2}[Y_s'(x,\pm 0) + Y_s'(x,-0)] = - \frac{1}{\pi} \int_0^1 \frac{[\Delta u(\xi) - \Delta u^2(\xi)/2]}{x - \xi} d\xi + I_c(x) \tag{16}$$

where

$$\Delta u^2(\xi) = [u^2(\xi,+0) - u^2(\xi,-0)]/2 \tag{17}$$

and

$$I_c(x) = - \frac{1}{4\pi} \int_S \int k_{\xi y}(x,\xi;0,\eta) [u^2(\xi,\eta) - \hat{u}^2(\xi)] dS \tag{18}$$

where

$$\hat{u}^2(\xi) = \begin{matrix} u^2(\xi,+0), & \eta > 0 \\ u^2(\xi,-0), & \eta < 0 \end{matrix} \tag{19}$$

is satisfied and that the Kutta condition of zero velocity jump at the trailing edge and on the wake is satisfied. In Equation (6)

$$Y_s(x,\pm 0) = k/\beta^3 \bar{Y}_s(x,\pm 0) \quad (7)$$

where $y = \bar{Y}_s(x,\pm 0)$ denotes the geometry of the airfoil on its upper and lower surfaces, respectively. $\bar{A}$ is given by

$$\bar{A} = k/\beta^3 \alpha \quad (8)$$

where α is the angle of attack, although it should be noted that in the formulation used in TSFOIL

$$\bar{A} = k/\beta^3 M_\infty^{-1/4} \alpha \quad (9)$$

The basic idea of the integral equation method is to use Green's theorem to write the differential equation, Equation (1), and its associated boundary conditions in integral form. A detailed description of the method is given in Reference 5.

For $y \neq 0$ the integral equation is given by

$$u - u^2/2 = u_{LS} + u_{LA} + I_T(u) \quad (10)$$

where

$$U_{LS}(x,y) = \frac{1}{2\pi} \int_0^1 [Y_s'(\xi,+0) - Y_s'(\xi,-0)] K_x(x,\xi;y,0)d\xi \quad (11)$$

and is the solution of Equation (1) without the nonlinear terms,

$$u_{LA}(x,y) = \frac{1}{\pi} \int_0^1 \Delta u(\xi) K_\eta(x,\xi;y,0)d\xi \quad (12)$$

stability terms used in algorithms tend to initiate the appearance of eigensolutions thus making the computations of a real solution different.

Since the behavior of the nonunique solutions is identical to that of the real solution the question arises as to whether these solutions are physically realizable. An analysis of the Navier-Stokes or, possibly, the Euler equations is necessary to determine this.

ACKKNOWLEDGEMENTS

Research sponsored by the Air Force Office of Scientific Research (AFSC) under contract F49620-79-C-0054 and by the Office of Naval Research under contract N00014-83-C-0056.

REFERENCES

1. Steinhoff, J. S. and Jameson, A.: Multiple Solutions of the Transonic Potential Flow Equation. AIAA Journal, Vol. 20, No. 11, 1982.

2. Salas, M.D., Gumbert, C. R., and Turkel, E.: Nonunique Solutions to the Transonic Potential Flow Equation. AIAA Journal, Vol. 22, No. 1, 1984.

3. Nixon, D.: Calculation of Transonic Flows Using an Extended Integral Equation Method. AIAA Journal, Vol. 15, No. 3, 1977.

4. Stahara, S. S.: Operational Manual for Two Dimensional Transonic Code TSFOIL. NASA CR 3064, 1978.

5. Nixon, D.: Calculation of Transonic Flows Using the Integral Equation Method. Ph.D. Thesis, University of London, England, 1976.

6. Nixon, D.: The Transonic Integral Equation Method with Curved Shock Waves. Acta Mechanica, Vol. 32/1-3, 1979.

7. Murman, E. M. and Cole, J. D.: Calculation of Plane Steady Transonic Flow. AIAA Journal, Vol. 9, No. 1, 1971.

8. Klopfer, G. H. and Nixon, D.: Non-Isentropic Potential Formulation for Transonic Flows. AIAA Journal, Vol. 22, No. 6, 1984.

APPENDIX

Further Comments On The Nature of Eigensolutions

It is possible that the only solution to Equation (27) is

$$f(\xi,\eta) = 0 \tag{A1}$$

In this case

$$\Delta u\ \bar{u} - \Delta u_o - I_{c_L} = 0 \tag{A2}$$

and

$$\Delta u_o = \frac{I_{cL}}{\bar{u}_o - 1} \tag{A3}$$

$$\Delta u = - I_{c_L} \frac{\bar{u}_o}{\bar{u}_o - 1} \Big/ \bar{u} \tag{A4}$$

If Equation (A2) is substituted into Equation (32) it follows that

$$\Delta u - \Delta u\ \bar{u} = \frac{1}{\pi} \int_o^1 \frac{I_{cL}(\xi)\ y}{(x-\xi)^2 + y^2}\, d\xi \tag{A4}$$

The right-hand side of equation (A5) can be recognized as Δu_L, the linear value of Δu in the flow field. Hence Equation (A5) becomes

$$\Delta u\ (1-\bar{u}) = \Delta u_L \tag{A6}$$

It can be seen that as $\bar{u} \to 1$ Δu becomes infinite which will give an expansion shock. Consequently, Equation (A1) cannot be the correct solution of Equation (32); a nonzero value of $f(\xi,\eta)$ must exist.

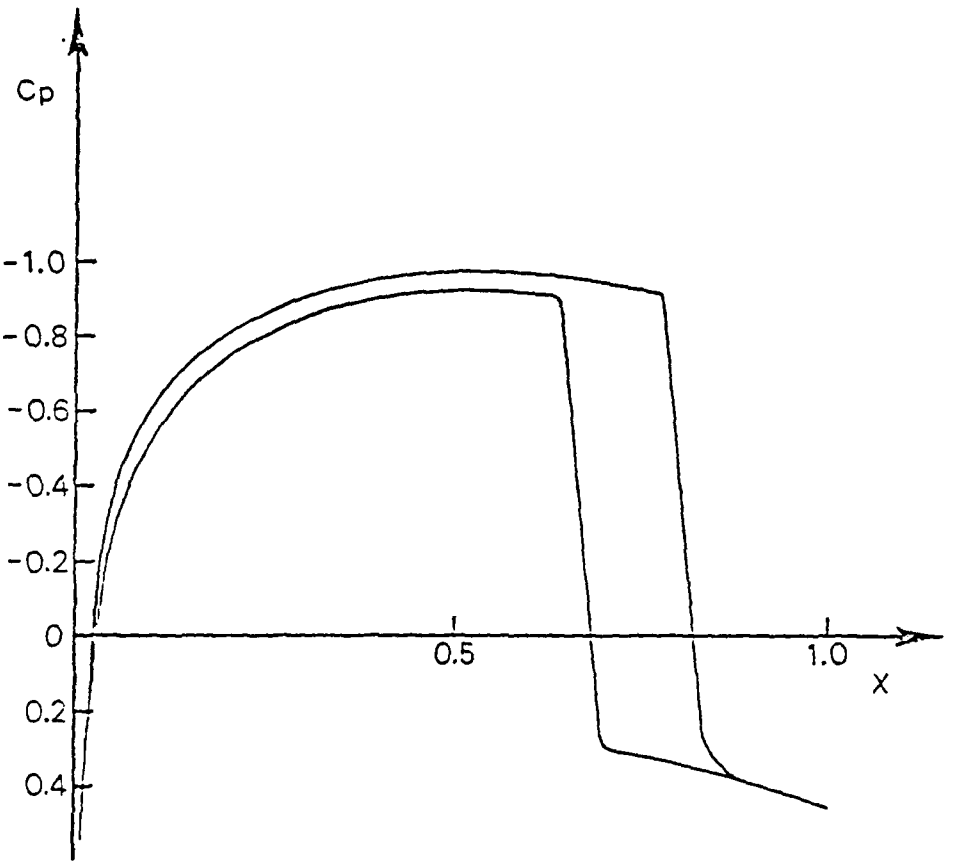

Figure 1.– Pressure distribution around a 11.8% Joukowski airfoil; $M_\infty = 0.85$, $\alpha = 0.0°$.

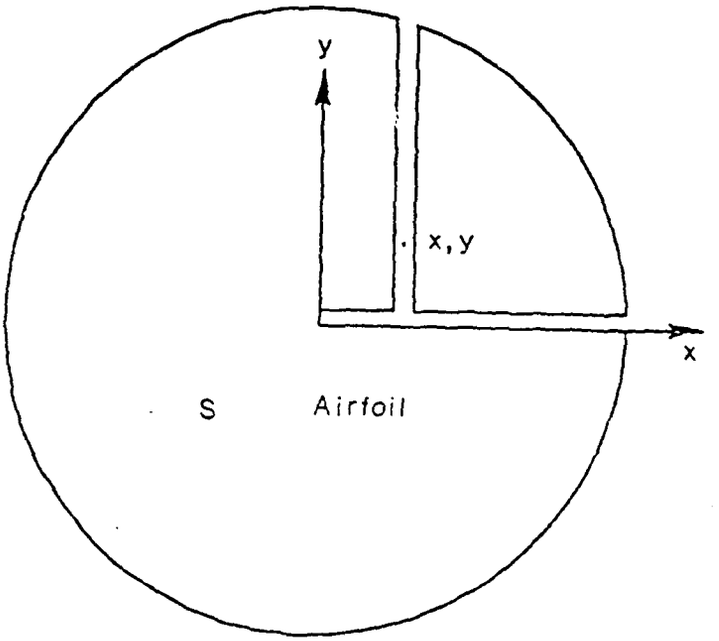

Figure 2 – Domain of integration S.

APPENDIX 3

Velocity Induced by a Moving Blade

The object is to estimate the induced upwash at some station y due to the oscillatory motion of a blade at y = 0. It is assumed that y is sufficiently far from the oscillating blade that linear theory can apply.

From classic subsonic theory the velocity potential in the far field is given by (see Reference 15)

$$\phi(x,\bar{y}) = \frac{\bar{A}}{(Kr)^{1/2}} \exp[-i(Kr-\tfrac{\pi}{4})] e^{iM_\infty^2 \Omega x} \tag{1}$$

where

$$r = (x^2 + \bar{y}^2)^{1/2} \tag{2}$$

and

$$K = \frac{M_\infty \nu}{1-M_\infty^2} \ , \ \bar{y} = (1-M_\infty^2)^{1/2} y \tag{3}$$

Far from the moving blade x can be taken as zero and, on differentiation with respect to y,

$$v(o,\bar{y}) = \frac{\bar{A}}{(1-M_\infty^2)^{1/2}} \frac{e^{i\pi/4}}{K^{1/2}} \{\frac{-1}{2\bar{y}^{3/2}} - \frac{iK}{\bar{y}^{1/2}}\} e^{iK\bar{y}} \tag{4}$$

as $\bar{y} \to \infty$, $v(o,\bar{y})$ can be approximated by

$$v(o,\bar{y}) = \frac{-i\bar{A}}{(1-M^2)^{1/2}} \frac{K^{1/2}}{\bar{y}^{1/2}} e^{iK\bar{y}} e^{i\pi/4} \tag{5}$$

$$= A \frac{e^{-iK\bar{y}}}{\bar{y}^{1/2}} \tag{6}$$

where $\bar{A}$ is a complex constant.

APPENDIX 4

by Alfred Ayoub

Convergence of the Series

$$\sum_{n=1}^{\infty} \frac{e^{in\alpha}}{n^{1/2}}$$

The convergence of the series $\sum_{n=1}^{\infty} \frac{e^{in\alpha}}{n^{1/2}}$ is due primarily to the cancellation effects provided by the term $e^{in\alpha}$, as the series $\sum_{n=1}^{\infty} \frac{1}{n^{1/2}}$ is divergent and therefore $\sum_{n=1}^{\infty} \frac{e^{in\alpha}}{n^{1/2}}$ is not absolutely convergent.

For values of α for which an integer p exists such that $p\alpha = \pi$, the series $\sum_{n=1}^{\infty} \frac{e^{in\alpha}}{n^{1/2}}$ can be reduced to an alternating series by grouping all consecutive terms of the same sign; the series that follows has monotonically decreasing terms and is therefore convergent.

While a somewhat similar approach can be followed for an arbitrary α, the procedure tends to become quite complex. The following proof of convergence on the other hand is more direct and exploits equally well the alternating character of $e^{in\alpha}$.

$$\sum_{n=1}^{\infty} \frac{e^{in\alpha}}{n^{1/2}} = e^{i\alpha} + \frac{e^{i2\alpha}}{2^{1/2}} + \ldots + \frac{e^{in\alpha}}{n^{1/2}} + \ldots$$

$$= (1 - \frac{1}{2^{1/2}})e^{i\alpha} + (\frac{1}{2^{1/2}} - \frac{1}{3^{1/2}})(e^{i\alpha} + e^{i2\alpha})$$

$$+ \ldots +$$

$$[\frac{1}{n^{1/2}} - \frac{1}{(n+1)^{1/2}}](e^{i\alpha} + \ldots + e^{in\alpha}) + \ldots$$

$$\text{or} \sum_{n=1}^{\infty} \frac{e^{in\alpha}}{n^{1/2}} = \sum_{n=1}^{\infty} \left[\frac{1}{n^{1/2}} - \frac{1}{(n+1)^{1/2}}\right] \quad (e^{i\alpha} + \ldots + e^{in\alpha})$$

The series on the right hand side of the above identity is absolutely convergent since:

$$\left| \left[\frac{1}{n^{1/2}} - \frac{1}{(n+1)^{1/2}}\right] \quad (e^{i\alpha} + \ldots + e^{in\alpha}) \right| < \frac{1}{2n^{3/2}} \left| \frac{1-e^{in\alpha}}{1-e^{i\alpha}}, \right|$$

$\sum_{n=1}^{\infty} \frac{1}{2n^{3/2}}$ is convergent (by Cauchy's integral test)

and $$\left| \frac{1-e^{in\alpha}}{1-e^{i\alpha}} \right| = \frac{\sin^2 n\alpha/2}{\sin^2 \alpha/2}$$

$$< \frac{1}{\sin^2 \alpha/2} \quad \text{finite and independent of M for } \alpha \neq 0, 2\pi, \ldots$$

It follows that the series

$$\sum_{n=1}^{\infty} \left[\frac{1}{n^{1/2}} - \frac{1}{(n+1)^{1/2}}\right] \quad (e^{i\alpha} + \ldots + e^{in\alpha})$$

is convergent and hence $\sum_{n=1}^{\infty} \frac{e^{in\alpha}}{n^{1/2}}$ is convergent.

It is interesting to note that the same proof above applies to all series of the form $\sum_{n=1}^{\infty} a_n b_n$ where $\sum_{n=1}^{\infty} b_n$ is bounded but not necessarily convergent and the terms a_n are all positive or all negative and a_n tends to zero monotonically as $\frac{1}{n^r}$ where r is any positive exponent.

END

DATE
FILMED
7-85

DTIC